5

Human Cadaver Patella-Femur-Pelvis Injury due to Dynamic Frontal Impact to the Patella

Richard M. Morgan
Rolf H. Eppinger
Jeffrey H. Marcus
U. S. DOT/NHTSA

Abstract

This study examined 126 unembalmed cadaver experiments in which the lower extremities are dynamically loaded. The injury data associated with the 126 cadaver leg impacts were examined to determine how well the existing femur injury criteria separate these specific cases. Most of the injuries were fractures although there were some traumas to ligaments and muscles. Statistical analysis was done on the 126 cadaver leg tests to associate injury (AIS number or injury/non-injury) with engineering parameters and anthropometric measurements recorded from the tests.

An analysis based on a 10 kN (2250 pound) applied femur force did a reasonable job of separating injury from non-injury. The 10 kN applied femur force point is estimated to represent a 35 % probability level of injury. A model did a better job of separating injury from non-injury for this data sample. The model separates injury by using both the maximum applied femur force and the rise time of that force, i. e., the time from initiation of force to when the maximum force occurs.

Introduction

Relative to patella-femur-pelvis injury, a body of research [1, 2, 3, 4, 5, 6][1] suggests that a reasonable femur injury criterion to prevent bone damage is to limit the axial compressive load to less than 10.0 kN (2250 pounds). Viano [7] suggested an 8.9 kN (2000 pounds) femur load be considered as a static portion of the criterion and that higher loads be allowed for cases where the duration of the femur force is less than 20 msec. In other words, Viano defined a permissible knee force as:

$$F_{max\ femur}(kN) = 23.14 - 0.71\ T_{pulse} \quad \text{when } T_{pulse} < 20 \text{ msec}$$

$$F_{max\ femur}(kN) = 8.90 \quad \text{when } T_{pulse} >= 20 \text{ msec}$$

Many of the data used in Reference 7 are pendulum impacts to the patella-femur-pelvis complex.

---

[1] Numbers in brackets designate references at end of paper.

Several investigators of impacts to the lower extremities of unembalmed human cadavers suggested that force alone may not be sufficient to always separate injury from non-injury. [3,5,8] In 1983, Leung et al. [8] presented the results of 16 cadaver tests performed in a vehicle body mounted on a sled. A formulation similar to the Viano criterion was found to separate injury from non-injury. The tolerance to fractures was found to depend on the cadaveric subject's bone condition. Cooke and Nagel [3] said the severity of trauma produced depended on both the peak forces generated and the impact energy absorbed. Melvin et al. also observed that -- for distal fractures of the femur and patella -- the peak axial force is not an adequate indicator of potential fracture and the kinetic energy level associated with the impact must be considered as well. They suggested peak force could be used in conjunction with the impulse -- where the assumption is the kinetic energy level can be inferred from the transferred momentum. Melvin et al. observed their fractures typically exhibited a single "sharp" load peak as shown in Figure 1 and non-fractures exhibited a "double peaked" wave form.

Procedure

The majority of the information used in this study is a subset taken from the National Highway Traffic Safety Administration's (NHTSA) Biomechanics Data Base. Over the past nine years, the agency has been systematically collecting the data from the biomechanical tests performed in different experimental programs and storing the information in one central repository. Currently, the total data bank holds the records of 599 human cadaver, 343 human volunteer, and 1370 dummy dynamic impacts conducted over 15 years from 1975 to 1989. The test type of the entire data bank ranges from component to whole body sled to vehicle crash tests while the impact direction varies mostly from anterior-posterior to medial-lateral. The experimental data (accelerometers, force, deflection, etc.) time histories are preserved on magnetic tape and read into the computer when needed for analysis. The files for the human cadaver tests include the necropsy record for each tests and Abbreviated Injury Scale (AIS) values as per the 1980 manual for each observed lesion. [9]

The tests selected for this study were dynamic frontal impacts to the patella of an unembalmed human cadaver. These tests were from four agency-sponsored studies.[10, 11, 12, 13, 14][2] and from two studies in the literature. [8, 15] The impacting device was either a pendulum or sled (details to follow).

Processing of Data Traces The purpose of this section is to discuss

---

[2]References 13 and 14 cover the same experiments.

four aspects of electronic data processing: type of transducers used, frequency content of data, quality screening, and the approaches taken to calculate the time duration of the force.

The analyses to be performed used electronic time histories collected during each test. These data include acceleration measured at the pelvis and the external force applied at the patella.

Every effort was made to use data which had SAE Class 1000 data specifications. The SAE recommended filter for the femur is Class 600. To the eyes of at least one of the authors, many of the SAE Class 600 femur force traces appeared "spiky" and looked like the "raw" traces (the SAE Class 1000 traces). Consequently, he won the argument; and all femur force data are processed with a Class 180 filter.

All data traces were screened for quality by: (1) checking to see if all specification data was correct and complete and (2) looking for traces that imply disagreement with physical principles, e. g. seeing if integration of the sled acceleration gave a value many times greater than the recorded sled velocity (in which cases the sled acceleration is suspect).

Many investigators in the literature (e. g., References 5, 7, 8, 12, 13, 14, and 17) found it beneficial to employ the primary pulse duration of the patella applied force (T_{pulse}) while investigating femur injury. The method used to determine the primary pulse duration appears to vary from study to study. To determine the primary pulse duration, Leung et al. [8] used an algorithm in which the impulse (integral of the applied femur force) is divided by the peak force as shown in Figure 2. Leung et al. termed the impulse divided by the maximum applied femur force (I/F_{max}) as the "conventional pulse duration." In other words, Leung et al. created a rectangle: (1) of height F_{max}, (2) of width equal to the "conventional pulse duration," and (3) of area equal to the area under the applied femur force curve. The "conventional pulse duration" is sensitive to the shape of the applied femur force curve. Donnelly et al. [12] used a primary pulse duration algorithm in which the peak is first determined; and then the times -- to the left side and right side of the peak force -- at 1/5th of the peak are determined. In the present study, the primary pulse duration is determined as the difference of the two times at 1/8th of the peak force as shown in Figure 3.[3] This primary pulse duration definition (1/8th) is sensitive to double peaks in the applied force

---

[3]We chose this specific value (1/8) because the 1/5th force value seemed to make the primary pulse duration unduly short in some cases. For the present data set, our computer algorithm was still robust when the two time marks were determined by 1/8th of the peak applied force. If the fraction is chosen slightly below 1/8th, the algorithm begins to fail, i. e., begins to choose the last data point as one of the time marks.

curves. This aspect of our definition of primary pulse duration shall be discussed later in an examination of experiments conducted at the University of California at San Diego.

The rise time -- see Figure 4 -- is defined simply as the difference of the time of maximum femur force and the time at 1/8th of the peak force (following initiation of impact).

The impulse, I, is the integration of the femur force from time of initiation of impact to time of completion of the applied femur force.

Description of Experimental Setups The experimental setup of the first of two cadaver sled test studies conducted at Wayne State University [10] is shown in Figure 5. The thoracic region was restrained by a nonventing air bag on a nonstroking column. The lower extremities were restrained by aluminum hexcel pads. Behind each separate aluminum hexcel pad was a uniaxial load cell which measured the force interaction with the patella (denoted as applied femur force herein). There was no internal load cell in the femoral shaft of the cadavers but there was a triaxial accelerometer mounted at the sacrum. A summary of the cadaver pendulum and sled tests is in Table 1. The cadaver experiments in the sled body of Figure 5 are identified in Tables 1 by a Test Number beginning with the letter 'A.'

The experimental setup of the second set of Wayne State University cadaver sled tests [11] is illustrated in Figure 6. The upper torso was restrained by a 2-point belt and each separate lower extremities hit a separate energy-absorbing knee bolster. Behind each distinct knee bolster was a 2-axis load cell whose output could be resolved into a resultant applied femur force. Each cadaver had a triaxial accelerometer mounted on the sacrum. The experiments in the sled body of Figure 6 are identified in Table 1 by a Test Number beginning with the letter 'W.'

At Calspan, each cadaver leg was separately impacted -- as illustrated in Figure 7 -- on the patella by a flat face pendulum. [12, 13] Each leg was struck separately in the pendulum experiments; unlike the sled trials in which both legs were loaded simultaneously. The applied femur load was determined from an accelerometer mounted on the pendulum. The cadavers had a triaxial accelerometer package on the sacrum. The pendulum experiments are denoted by the letter 'C' in Table 1.

The cadaver sled tests performed at the University of California at San Diego (UCSD) [14] were conducted in a sled buck -- shown in Figure 8 -- which is based on a 1983 Chevrolet Citation. Each lower extremity of the "unrestrained" occupant was controlled separately by deformable blocks of semirigid polyurethane foam. Behind both the right and left foam block were three uniaxial load cells from which a resultant applied femur load was computed. The cadavers had a pelvic triaxial accelerometer mount. The UCSD sled tests are denoted by the

letter 'S' in Table 1. The UCSD data in Table 1 exhibits great differences in the primary pulse duration for similar test conditions. This variation is caused by the fact our primary pulse duration sometimes spans single and sometimes multiple peaks.

In 1980, four unembalmed cadaver sled tests were performed at the University of Michigan [15] where the seated subject slid forward during sled deceleration and the patella hit an impact surface. The test configuration is illustrated in Figure 9. Behind the surface were two load cells, each in line with a right or left leg respectively. The first test had 2.54-cm of Ensolite. The second test had 5.08-cm of Ensolite. The third: 2.54-cm of Ensolite backed by 2.54-cm of polystyrene foam. The fourth: 2.54-cm of Ensolite backed by 5.08-cm of polystyrene foam. The cadavers had a triaxial accelerometer on the sacrum. The University of Michigan sled tests are indicated by the letter 'M' in Table 1.

The tests in Reference 8 were sled tests with a European car model and 2-point and 3-point belted unembalmed cadavers. The cadavers were positioned in the front seat passenger position as shown in Figure 10. A plane rigid disk covered with 2.5-cm of polyurethane was positioned in front of each separate leg. A separate measurement device was positioned behind each "knee bolster" disk to measure the normal component of the impact load. In this way, independent applied force loads for each leg were obtained. The cadavers had a triaxial accelerometer on the pelvis. The Peugeot-Renault Association sled tests are indicated by the letter "F" in Table 1.

As discussed in the section above, every effort was made to examine the experiments for quality of data. For example, the integral of the applied femur force was checked against an approximate change of momentum. However, there is no guarantee the cadaveric femur shaft was always aligned with the pertinent load cell axis all the time in all these variegated experiments. In addition, different instruments were used at the various laboratories to determine the applied force. For the force curves which passed the quality control check and were used in this paper, the assumption is made that the variation due to femur-load-cell alignment and due to data collection differences is less than the variation in the response of the biological specimens.

Summary of Injuries Produced in Laboratory Experiments The first and second highest AIS numbers -- for the lower extremity injuries of the 126
cadaver leg impact tests -- are found in Table 1. A detailed written description of all the lower extremity injuries resulting from the 126 cadaver leg impacts is in Appendix A.

The 16 cadaver legs -- impacted in the sled shown in Figure 5 -- were not injured.

Twenty of the 22 cadaver legs impacted in the sled shown in Figure 6 were also not injured. One subject received multiple fractures at

the distal end of both femur.

For the Calspan pendulum tests depicted in Figure 7, 25 out of 30 lower extremities were injured. When the rigid face pendulum initial velocity was nominally 14.5-km/hr, three legs were uninjured and one had ligament tears at the knee joint. For a pendulum (rigid and padded faces depending on the particular test) velocity of 26- to 29-km/hr, 18 out of 20 lower extremities were injured. Most of the injuries could be characterized as one or more fractures in the knee area with an occasional injury in the proximal femur region. For padded face pendulum experiments at about 40-km/hr, six of six legs were injured. These injuries could be characterized as multiple fractures all around the patella and distal femur region with some muscle lacerations.

In the 24- to 40-km/hr initial velocity sled tests conducted at the University of California at San Diego -- see Figure 8 -- only one out of 21 legs were injured. This single injury was a deep laceration of the skin over the knee.

For the sled tests conducted at the University of Michigan -- see Figure 9 -- six out of eight cadaver legs were injured. The injuries could be loosely described as more than one fracture located at one or more of the patella, femur condyles, femur shaft, or femur head.

For the sled tests of Reference 8 -- shown in Figure 10 -- six out of 29 cadaver legs were injured. The injuries could be described as fractures to the patella or femur condyles with one femur neck fracture.

In summary, while pendulum tests account for only 24 % of the experiments, they represent 63 % of the injuries. In addition, the Table 1 data sample does not possess a solitary femoral shaft fracture without injury to the patella or femoral condyles, which solitary type of injury is reported in real world collisions. [18] It appears the Table 1 data sample is more representative of the kind of injury which occurs when the knee impacts stiff, unyielding structures.

Analysis of Patella-Femur-Pelvis Injuries Figure 11 is a graph of injury/non-injury versus maximum applied femur force. There is a region of lower values of force for which there are no lower extremity injuries. Next, there is a relative long transition region in which both injuries
and non-injuries are observed. Lastly, non-injuries disappear for the higher force values. So, maximum applied femur force alone is not a perfect injury index -- i. e., there is an overlap of some 54 % of the data points in a transition region. A probability of injury -- based on applied femur force as the lone independent variable -- was developed using a Weibull distribution and the Maximum Likelihood Method and is presented in Figure 12. [19, 20] A force value of 10 kN (2250 pounds) appears to be at the 35 % level of injury risk.

Figure 12 (the Weibull Function) shows a curve -- a steadily rising curve having a sigmoidal shape -- which gives the fraction of the population which has responded to an exposure. Figure 13 is the derivative of the Weibull Function and should be interpreted such that the area between any two abscissa represents the proportion of the population having tolerances between these two abscissas, i. e., Figure 13 is the underlying population distribution. (Figure 13 is called the probability density function by statisticians. Integration of the entire area under the curve in Figure 13 should sum to one.) The underlying population distribution appears reasonably normal in shape for the choice of applied femur force as the sole independent variable.

A model in Figure 14 shows maximum applied femur force plotted versus the rise time of the applied femur force. The cadaver injury data displayed in Figure 14 was next analyzed by multiple discriminant analysis for the data subsample in which $T_{Rise\ Time}$ is < = 10 msec. [21, 22] The reason for using a subsample was there is no injury in the entire data sample for $T_{Rise\ Time}$ > 10 msec.

Discriminant analysis is an appropriate statistical technique when the dependent variable is categorical. When a value is assigned to a categorical variable, it serves merely as a label or means of identification, e. g., 0 for male and 1 for female. Discriminant analysis involves finding the best linear combination of the two (or more) independent variables (which will generally have a constant unit of measurement but may be a categorical variable just like the categorical dependent variable) that will discriminate best between the two (or more) categories of the dependent variable. This is accomplished by statistically maximizing the between group variance and minimizing the within group variance. The linear combinations used in the discriminant analysis take the following form:

$$Z = W_1 X_1 + W_2 X_2$$

where

Z = the discriminant score,

W = the discriminant weights,

and

X = the independent variables.

Figure 15 plots injury versus the best -- in the Discriminant Analysis sense -- linear combination of maximum applied femur force and rise time for the data subsample where $T_{Rise\ Time}$ < = 10 msec. The transition region -- i. e., the overlap where both injury and non-injury happen -- covers only 41 % of all the data points.

Using a Weibull distribution and the Maximum Likelihood Method, the probability of injury based on the linear combination of applied femur force and rise time -- for $T_{Rise\ Time}$ < = 10 msec -- was

computed for Figure 16.

For $T_{Rise\ Time}$ < = 10 msec in Figure 14, the probability curve of Figure 16 was used to define a 50 % probability of injury line. Note that the 50 % line seems to divide the cadaver impact data into three regions: (1) a portion in the middle to upper left hand side where there are mostly injuries, (2) a portion along the bottom where there are mostly non-injuries, and (3) a portion in the middle where there are no data points.

There is a hypothesis which would explain why the center portion is without data points. Early in our analysis of the 112 cadaver leg impact curves, we observed we had the same shape dependence as found by Melvin et al. in Figure 1: the injury cases had a "spike" shaped curve while the non-injury cases had a more "spread-out" shape. (This is a general observation and not true in each and ever case.) Were a hypothetical cadaver to be impacted such that it had no injury and its hypothetical force curve put it at the bottom of Figure 14, then we could imagine a succession of abstract cadaver impacts in which the curve shape stayed the same but applied femur force and rise time increased. Since force is increasing and absorbed energy is increasing, one of these successive hypothetical cadavers must eventually break a leg according to Cooke and Nagel. But, for whichever hypothetical cadaver is first injured, the actual measured force time history -- according to Melvin et al. and the 112 experiments of Table 1 -- may not have the same wave shape as the preceding abstract cadavers. Once the injury occurs, the actual measured force may fall off more sharply as shown in the first curve of Figure 1. To complete the hypothesis, the actual measured force would be such that the last hypothetical cadaver experiment would drop in the region to the left in Figure 14. Future lower extremity research might test this hypothesis by attempting to run experiments which fall in the center region of Figure 14.

After 10 msec, where does the 50 % probability line go ? Since there are no injuries after 10 msec for this data set, the non-injury region was arbitrarily capped by a horizontal femur force line at F_{max} = 14.6 kN. A similar design was constructed in Figure 14 for the 21 % probability line which is capped at 12 kN.

A grouping of the data based on both (1) the maximum applied femur force and (2) the primary pulse duration of the applied femur force -- as suggested by some researchers -- failed to separate injury from non-injury for this data set. See Appendix B for details.

Conclusions

o This study examined the results of 126 impacts to the lower extremities of human cadavers for the purpose of predicting injury/non-injury. Applied femur force alone did a reasonably good job of separating injury/non-injury although there was a large region of injury/non-injury overlap (54 % of the data points fell in the transition region). The 10 kN force point is estimated to represent

the 35 % level of injury.

o Using applied femur force and the femur force primary pulse duration -- for examination of this data set -- led to no better discrimination of injury/non-injury for this data sample than femur force alone.

o When the maximum applied femur force and rise time were considered, a better discrimination capability between injury/non-injuries was obtained, i. e., about 41 % of the data points fell in the injury/non-injury overlap region using this formulation. The model suggests that the peak force associated with injury is lower for short rise times than for longer rise times and is contrary to conclusions of previous investigations.

Acknowledgments Special thanks goes to Dr. Claude Tarriere and the research team associated with Peugeot-Renault Association (France). They gave us copies of their data curves produced in 16 human cadaver sled tests (circa 1983). The data was very valuable to this current study.

Disclaimer The views presented are those of the authors and are not necessarily those of the National Highway Traffic Safety Administration, U. S. Department of Transportation.

References

1. Patrick, L. M., Kroell, C. K., and Mertz, H. J., "Forces on the Human Body in Simulated Crashes," Ninth Stapp Car Crash Conference Proceedings, 1965.

2. Patrick, L. M., Mertz, H. J., and Kroell, C. K., "Cadaver Knee Chest and Head Impact Loads," Eleventh Stapp Car Crash Conference Proceedings, October 1967.

3. Cooke, F. W., and Nagel, D. A., "Biomechanical Analysis of Knee Impact," Thirteenth Stapp Car Crash Conference Proceedings, December 1969.

4. Powell, W. R., Advani, S. H., Clark, R. N., Ojala, S. J., and Holt, D. J., "Investigation of Femur Response to Longitudinal Impact," Eighteenth Stapp Car Crash Conference Proceedings, December 1974.

5. Melvin, J. W., Stalnaker, R. L., Alem, N. M., Benson, J. B., and Mohan, D., "Impact Responses and Tolerance of the Lower Extremities," Nineteenth Stapp Car Crash Conference Proceedings, November 1975.

6. Powell, W. R., Ojala, S. J., Advani, S. H., and Martin, R. B.,

"Cadaver Femur Responses to Longitudinal Impacts," Nineteenth Stapp Car Crash Conference Proceedings, November 1975.

7. Viano, D. C., "Considerations for a Femur Injury Criterion," Twenty-First Stapp Car Crash Conference Proceedings, October 1977.

8. Leung, Y. C., Hue, B., Fayon, A., Tarriere, C., Hamon, H., Got, C., Patel, A., and Hureau, J., "Study of 'Knee-Thigh-Hip' Protection Criterion," Twenty-Seventh Stapp Car Crash Conference Proceedings with International Research Committee on Biokinetics of Impacts, October 1983.

9. The Abbreviated Injury Scale, American Association for Automotive Medicine, Morton Grove, Illinois, 1980 Revision.

10. Cheng, R., Yang, K. H., Levine, R. S., King, A. I., and Morgan, R., "Injuries to the Cervical Spine Caused by a Distributed Frontal Load to the Chest," Twenty-Sixth Stapp Car Crash Conference Proceedings, October 1982.

11. Cheng, R., Yang, K., Levine, R. S., and King, A. I., "Dynamic Impact Loading of the Femur Under Passive Restrained Condition," Twenty-Eighth Stapp Car Crash Conference Proceedings, November 1984.

12. Roberts, D. P., Donnelly, B. R., and Morgan, R., "Cadaver Response to Axial Impacts of the Femur," Eleventh International Technical Conference on Experimental Safety Vehicles, May 1987.

13. Donnelly, B. R., and Roberts, D. P., "Comparison of Cadaver and Hybrid III Dummy Response to Axial Impacts of the Femur," Thirty-First Stapp Car Crash Conference Proceedings, November 1987.

14. Morgan, R. M., Schneider, D. C., Eppinger, R. H., Nahum, A. M., Marcus, J. H., Awad, J., Dainty, D., and Forrest, S., "Interaction of Human Cadaver and Hybrid III Subjects with a Steering Assembly," Thirty-First Stapp Car Crash Conference Proceedings, November 1987.

15. Melvin, J. W., and Nusholtz, G. S., "Tolerance and Response of the Knee-Femur-Pelvis Complex to Axial Impacts: Impact Sled Tests," University of Michigan, Highway Safety Research Institute, Ann Arbor, Report No. UM-HSRI-80-27, 1980.

16. Viano, D. C., "Femoral Impact Response and Fracture," Fifth International IRCOBI Conference on the Biomechanics of Impact, September 1980.

17. Viano, D. C., Culver, C. C., Haut, R. C., Melvin, J. W., Bender, M., Culver, R. H., and Levine, R. S., "Bolster Impacts to the Knee and Tibia of Human Cadavers and an Anthropomorphic Dummy," Twenty-Second Stapp Car Crash Conference Proceedings, October 1978.

18. States, J. D., "Adult Occupant Injuries of the Lower Limb," SAE Paper No. 861927, Symposium on Biomechanics and Medical Aspects

of Lower Limb Injuries, October 1986.

19. Ran, A., Koch, M. and Mellander, H., "Fitting Injury Versus Exposure Data into a Risk Function," International IRCOBI Conference on the Biomechanics of Impacts, September 1984.

20. Koch, M., "Recent Work with a Method for the Fitting of Injury Versus Exposure Data into a Risk Function," International IRCOBI Conference on the Biomechanics of Impacts, September 1988.

21. Hair, J. F., Anderson, R. E., and Tatham, R. L., Multivariate Data Analysis with Readings, Macmillan Publishing Company, New York, 1987.

22. SAS Institute, Inc., SAS User's Guide: Statistics, Version 5, Cary, N. C., 1985.

Table 1 - Summary of Cadaver Data

Test Number	Test Type	Mass (kg)	Age (yrs)	Stature (cm)	Applied Femur Force (kN)	Applied Femur Impulse (kN*sec)	Time Period 12.5% (msecs)	Applied Femur Rise Time (msecs)	Pelvis Acc Resultant (g's)	Pelvis Velocity (km/hr)	Time Period 12.5% (msecs)	AIS 1	AIS 2	Delta V (km/hr)
WAYNE STATE UNIVERSITY (Figure 4 and Ref. 10)														
A81022	BAG	72.7	66	170.2	7.94	0.194	45	33.1	61.1	72	65.0	0	0	47
A81122	BAG	72.7	66	170.2	8.68	0.207	46.3	33.8	61.1	72	65.0	0	0	47
A81026	BAG	50	54	152.4	5.45	0.119	38.8	10	66.3	89	78.0	0	0	47
A81126	BAG	50	54	152.4	4.25	0.100	36.9	2.5	66.3	89	78.0	0	0	47
A81032	BAG	96.3	56	185.4	10.22	0.236	37.5	10.6	114	80	68.0	0	0	47
A81132	BAG	96.3	56	185.4	10.40	0.175	29.4	8.8	114	80	68.0	0	0	47
A81035	BAG	74.0	63	180.3	12.28	0.211	24.4	9.4	150.9	116	60.0	0	0	49
A81135	BAG	74.0	63	180.3	11.67	0.186	23.1	10	150.9	116	60.0	0	0	49
A82038	BAG	83.1	68	175.3	11.00	0.271	35	9.4	124.3	109	50.0	0	0	48
A82138	BAG	83.1	68	175.3	10.37	0.245	34.4	11.3	124.3	109	50.0	0	0	48
A82039	BAG	60	67	175.3	9.18	0.139	21.3	6.3	187.9	89	47.0	0	0	48
A82139	BAG	60	67	175.3	8.18	0.138	23.1	10	187.9	89	47.0	0	0	48
A82040	BAG	87.7	61	167.6	7.08	0.193	38.5	5.5	81.3	71	60.0	0	0	48
A82140	BAG	87.7	61	167.6	6.86	0.162	37.5	6	81.3	71	60.0	0	0	48
A82041	BAG	60.9	66	177.8	8.85	0.217	40.5	6	102.9	90	61.0	0	0	48
A82141	BAG	60.9	66	177.8	7.63	0.192	39.5	7	102.9	90	61.0	0	0	48
WAYNE STATE UNIVERSITY (Figure 5 and Ref. 11)														
W83015	100	67.2	46	162.6	NA	NA	NA	NA	78.2	64	55.0	0	0	46
W83115	100	67.2	46	162.6	6.94	0.121	28.5	10	78.2	64	55.0	0	0	46
W83016	100	80.9	60	175.3	9.08	0.234	48	11	65.1	60	34.0	0	0	47
W83116	100	80.9	60	175.3	8.23	0.178	43	12	65.1	60	34.0	0	0	47
W83018	100	60	21	170.2	9.35	0.262	52.5	12	NA	NA	NA	0	0	47
W83118	100	60	21	170.2	9.16	0.198	26	12.5	NA	NA	NA	0	0	47
W83019	LKB	56.3	65	167.6	6.31	0.121	33.5	17.5	57.6	63	45.5	0	0	43
W83119	LKB	56.3	65	167.6	NA	NA	NA	NA	57.6	63	45.5	0	0	43
W83020	100	95.9	29	175.3	9.75	0.316	62	11	68.4	68	66.0	0	0	50
W83120	100	95.9	29	175.3	10.97	0.416	78	20	68.4	68	66.0	0	0	50
W83021	60	51.3	56	152.4	10.42	0.222	29.5	15	105.8	77	26.0	0	0	47
W83121	60	51.3	56	152.4	5.94	0.104	24	11.5	105.8	77	26.0	0	0	47
W84023	60h	70.4	63	172.7	10.60	0.222	21.5	13.5	64.1	82	82.0	0	0	45
W84123	60h	70.4	63	172.7	7.86	0.183	39	11.5	64.1	82	82.0	0	0	45
W84024	60h	80.4	58	162.6	10.08	0.251	32.5	5.5	81.1	77	66.0	3	2	45
W84124	60h	80.4	58	162.6	9.27	0.210	18.5	9.5	81.1	77	66.0	3	0	45
W84025	60h	74.5	58	172.7	10.09	0.234	43	9.5	81.4	71	48.5	0	0	47
W84125	60h	74.5	58	172.7	12.25	0.251	48	13.5	81.4	71	48.5	0	0	47
W84026	60h	52.2	63	175.3	8.21	0.157	20	10.5	158.2	84	29.5	0	0	53
W84126	60h	52.2	63	175.3	10.33	0.210	19.5	10	158.2	84	29.5	0	0	53
W85027	SLN	73.1	61	170.2	14.02	0.287	22.5	9.5	132.1	80	19.5	0	0	51
W85127	SLN	73.1	61	170.2	11.26	0.307	43	9.5	132.1	80	19.5	0	0	51

Table 1 - Summary of Cadaver Data

Test Number	Test Type	Mass (kg)	Age (yrs)	Stature (cm)	Applied Femur Force (kN)	Applied Femur Impulse (kN*sec)	Time Period 12.5% (msecs)	Applied Femur Rise Time (msecs)	Pelvis Acc Resultant (g's)	Pelvis Velocity (km/hr)	Time Period 12.5% (msecs)	AIS 1	AIS 2	Delta V (km/hr)
CALSPAN CORPORATION (Figure 6 and Ref. 12 and 13)														
C84025	PENR	85.4	55	182.9	NA	NA	NA	NA	69	13	8.0	0	0	14
C84125	PENR	85.4	55	182.9	NA	NA	NA	NA	73	14	10.0	0	0	14
C84029	PENR	68.6	71	170.2	9.33	0.057	12	1.1	195	16	9.0	0	0	14
C84129	PENR	68.6	71	170.2	7.02	0.055	14	3.2	147	23	7.0	3	2	15
C84030	PENR	84.0	66	175.3	18.66	0.077	6	1.2	189	31	8.0	2	0	28
C84130	PENR	84.0	66	175.3	18.13	0.107	12	3.1	248	26	9.0	2	0	27
C84031	PENR	73.1	57	170.2	14.06	0.089	12	3.8	255	37	8.0	2	0	26
C84131	PENR	73.1	57	170.2	13.29	0.082	11	3.4	258	48	9.0	2	0	27
C84032	PENR	57.2	60	165.1	8.55	0.063	11	1.7	203	37	8.0	3	2	27
C84132	PENR	57.2	60	165.1	7.73	0.062	14	3	205	27	6.0	2	0	27
C84033	PENR	59.5	70	170.2	9.40	0.070	12	4.3	163	31	6.0	3	2	27
C84133	PENR	59.5	70	170.2	7.91	0.070	15	5	142	31	7.0	2	0	27
C84034	PENR	64.0	55	180.3	21.06	0.125	11	1.2	219	31	8.0	2	2	28
C84134	PENR	64.0	55	180.3	19.68	0.143	18	1.8	135	19	5.0	3	0	28
C84035	PENR	68.1	69	175.3	11.39	0.081	10	3.2	186	29	10.0	3	2	28
C84135	PENR	68.1	69	175.3	15.13	0.098	11	2.5	233	31	5.0	2	2	28
C84036	PENP	72.7	61	175.3	17.18	0.081	9	3.3	213	34	10.0	2	2	28
C84136	PENP	72.7	61	175.3	10.89	0.089	20	5.4	155	27	6.0	2	2	28
C85037	PENP	46.8	57	157.5	9.34	0.076	19	6.2	120	43	40.0	2	2	28
C85137	PENP	46.8	57	157.5	8.99	0.071	14	5	140	35	20.0	3	2	28
C85038	PENP	44.0	49	157.5	NA	NA	NA	NA	109	26	6.0	3	0	28
C85138	PENP	44.0	49	157.5	NA	NA	NA	NA	129	24	6.0	2	0	28
C85039	PENP	70.4	65	167.6	NA	NA	NA	NA	120	32	14.0	0	0	28
C85139	PENP	70.4	65	167.6	NA	NA	NA	NA	123	31	13.0	0	0	28
C85040	PENP	84.0	66	185.4	NA	NA	NA	NA	333	56	14.0	3	2	40
C85140	PENP	84.0	66	185.4	NA	NA	NA	NA	249	40	9.0	3	2	40
C85041	PENP	79.5	62	182.9	10.01	0.072	28	2.8	235	31	7.0	3	3	40
C85141	PENP	79.5	62	182.9	14.19	0.102	16	2.8	304	43	5.0	3	3	43
C85042	PENP	86.3	60	172.7	11.60	0.107	37	2.9	329	51	7.0	3	3	40
C85142	PENP	86.3	60	172.7	11.88	0.068	14	2.5	311	47	8.0	3	3	40

Table 1 - Summary of Cadaver Data

Test Number	Test Type	Mass (kg)	Age (yrs)	Stature (cm)	Applied Femur Force (kN)	Applied Femur Impulse (kN*sec)	Time Period 12.5% (msecs)	Applied Femur Rise Time (msecs)	Pelvis Acc Resultant (g's)	Pelvis Velocity (km/hr)	Time Period 12.5% (msecs)	AIS 1	AIS 2	Delta V (km/hr)
UNIVERSITY OF CALIFORNIA AT SAN DIEGO (Figure 7 and Ref. 14)														
S85020	SW	54.5	79	170.2	0.93	0.027	47.3	7.5	14.2	35	85.0	0	0	25
S85120	SW	54.5	79	170.2	2.13	0.140	104.6	22.7	14.2	35	73.0	0	0	25
S85022	SW	78.6	74	185.4	2.51	0.102	74.1	22.4	18.9	37	89.0	0	0	23
S85122	SW	78.6	74	185.4	2.70	0.124	81	25.4	18.9	37	89.0	0	0	23
S85023	SW	77.2	68	172.7	3.25	0.110	73	17.6	23.5	39	78.0	0	0	24
S85123	SW	77.2	68	172.7	2.69	0.110	73.6	17.4	23.5	39	78.0	0	0	24
S85024	SW	70.4	75	177.8	3.22	0.127	47	18.7	30.9	49	75.0	0	0	34
S85124	SW	70.4	75	177.8	2.37	0.081	58.5	11	30.9	49	75.0	0	0	34
S86001	SW	58.1	74	175.3	7.24	0.329	62.9	38.9	37.3	58	73.0	0	0	40
S86101	SW	58.1	74	175.3	4.11	0.117	34.5	13.3	37.3	58	40.3	0	0	40
S86002	SW	53.1	60	152.4	8.63	0.242	57.4	37.9	71.3	53	40.3	0	0	46
S86003	SW	66.8	71	167.6	NA	NA	NA	NA	37.3	64	72.0	0	0	44
S86103	SW	66.8	71	167.6	NA	NA	NA	NA	37.3	64	72.0	2	0	44
S86004	SW	59.0	56	172.7	2.09	0.084	65.6	11.5	45.3	64	76.2	0	0	44
S86104	SW	59.0	56	172.7	6.66	0.223	74.7	27.1	45.3	64	76.0	0	0	44
S86005	SW	76.3	72	177.8	4.91	0.262	78.4	14.5	31.9	64	72.0	0	0	43
S86105	SW	76.3	72	177.8	4.56	0.201	67.3	30.1	31.9	64	72.0	0	0	43
S86007	SW	57.2	54	172.7	6.79	0.265	73.6	44.6	80.5	60	68.0	0	0	44
S86107	SW	57.2	54	172.7	4.18	0.047	13.6	2.3	80.5	60	68.0	0	0	44
S86008	SW	68.1	62	177.8	6.39	0.262	58.3	22.3	NA	NA	NA	0	0	44
S86108	SW	68.1	62	177.8	2.26	0.061	27.6	15.4	NA	NA	NA	0	0	44
UNIVERSITY OF MICHIGAN (Figure 8 and Ref. 15)														
M80018	S	77.2	75	177.8	12.99	0.076	7.2	1.9	243.2	45	11.3	3	3	30
M80118	S	77.2	75	177.8	21.70	0.171	17.8	4.4	243.2	45	11.3	3	3	30
M80020	S	86.8	49	188.0	18.21	0.157	12.6	2.4	350	87	12.8	3	3	34
M80120	S	86.8	49	188.0	21.73	0.196	14.3	6.6	350	87	12.8	3	3	34
M80021	S	83.1	79	NA	20.75	0.157	15.4	4.5	144.7	31	9.9	3	3	33
M80121	S	83.1	79	NA	18.84	0.152	12.8	5.9	144.7	31	9.9	3	2	33
M80022	S	46.8	58	157.5	6.35	0.131	31.5	10.5	67.8	27	17.8	0	0	34
M80122	S	46.8	58	157.5	8.60	0.154	25.6	10.5	67.8	27	17.8	0	0	34

Table 1 - Summary of Cadaver Data

Test Number	Test Type	Mass (kg)	Age (yrs)	Stature (cm)	Applied Femur Force (kN)	Applied Femur Impulse (kN*sec)	Time Period 12.5% (msecs)	Applied Femur Rise Time (msecs)	Pelvis Acc Resultant (g's)	Pelvis Velocity (km/hr)	Time Period 12.5% (msecs)	AIS 1	AIS 2	Delta V (km/hr)
PEUGEOT-RENAULT ASSOCIATION (FRANCE) (Figure 9 and Ref. 8)														
F0224	3PT	40	34	160.0	1.26	0.007	11	8.8	53.6	71	70.0	0	0	51
F1224	3PT	40	34	160.0	2.97	0.012	7.5	3.1	53.6	71	70.0	0	0	51
F0231	3PT	60.9	60	165.1	6.09	0.103	41.7	3.4	111.3	84	49.0	0	0	51
F1231	3PT	60.9	60	165.1	2.41	0.036	29.8	5.5	111.3	84	49.0	0	0	51
F0232	3PT	49.0	57	162.6	7.15	0.118	31.2	6.5	117.8	100	50.0	0	0	51
F1232	3PT	49.0	57	162.6	3.30	0.021	11.7	2.8	117.8	100	50.0	0	0	51
F0254	3PT	51.8	63	162.6	6.00	0.060	11.6	5.6	97.5	80	47.0	0	0	42
F1254	3PT	51.8	63	162.6	6.91	0.064	15.1	4.5	97.5	80	47.0	0	0	42
F0255	3PT	55.9	68	165.1	8.09	0.154	28.4	8.2	87.2	74	56.0	0	0	51
F1255	3PT	55.9	68	165.1	7.28	0.100	28.6	8.4	87.2	74	56.0	0	0	51
F0257	3PT	51.8	42	154.9	2.28	0.014	9.6	3.3	65.4	64	61.0	0	0	68
F1257	3PT	51.8	42	154.9	3.16	0.030	21.7	6.1	65.4	64	61.0	0	0	68
F0258	3PT	64.0	42	165.1	7.45	0.142	36.6	3.4	136.6	61	29.0	0	0	64
F1258	3PT	64.0	42	165.1	5.68	0.088	25.2	3.4	136.6	61	29.0	0	0	64
F0267	3PT	70.9	68	165.1	8.12	0.169	45.4	7.7	79.3	64	39.0	0	0	60
F1267	3PT	70.9	68	165.1	5.39	0.073	21.7	5.3	79.3	64	39.0	0	0	60
F1268	3PT	65.9	62	172.7	5.50	0.100	35.9	7	90.2	89	72.0	0	0	68
F0276	3PT	81.8	55	180.3	7.80	0.146	43.9	6.3	86.9	89	52.0	0	0	64
F1276	3PT	81.8	55	180.3	5.42	0.071	24.8	6	86.9	89	52.0	0	0	64
F0277	3PT	50	52	165.1	3.64	0.036	24.8	4.4	97.5	90	53.0	0	0	68
F1277	3PT	50	52	165.1	2.49	0.022	19.1	7.6	97.5	90	53.0	0	0	68
F0280	2PT	77.7	62	175.3	12.53	0.391	66.8	7.8	84.2	93	65.0	3	2	69
F1280	2PT	77.7	62	175.3	10.60	0.174	25.2	5.4	84.2	93	65.0	2	0	69
F0281	2PT	63.1	73	165.1	7.73	0.164	39	6.1	151.2	103	57.0	3	2	66
F1281	2PT	63.1	73	165.1	9.10	0.196	51.6	7.7	151.2	103	57.0	2	0	66
F0294	2PT	69.0	71	165.1	11.26	0.182	34.4	3.8	164.9	113	52.0	3	0	69
F1294	2PT	69.0	71	165.1	11.56	0.347	69.3	10.6	164.9	113	52.0	0	0	69
F0296	2PT	68.1	55	170.2	NA	NA	NA	NA	120.1	74	40.0	0	0	64
F1296	2PT	68.1	55	170.2	NA	NA	NA	NA	120.1	74	40.0	3	3	64

Bag = Sled test with non-venting bag
100 = 100-deg knee angle run at 22g's
LKB = Low knee bolster at 100-deg angle
60 = 60-deg knee angle run at 22g's
60h = 60-deg knee angle run at 35g's
PENR = Pendulum Rigid
PENP = Pendulum Padded
SW = Energy absorbing steering wheel
S = Sled with harness and adjustable knee impact surface
2PT = Sled with vehicle body and 2 point belt
3PT = Sled with vehicle body and 3 point belt

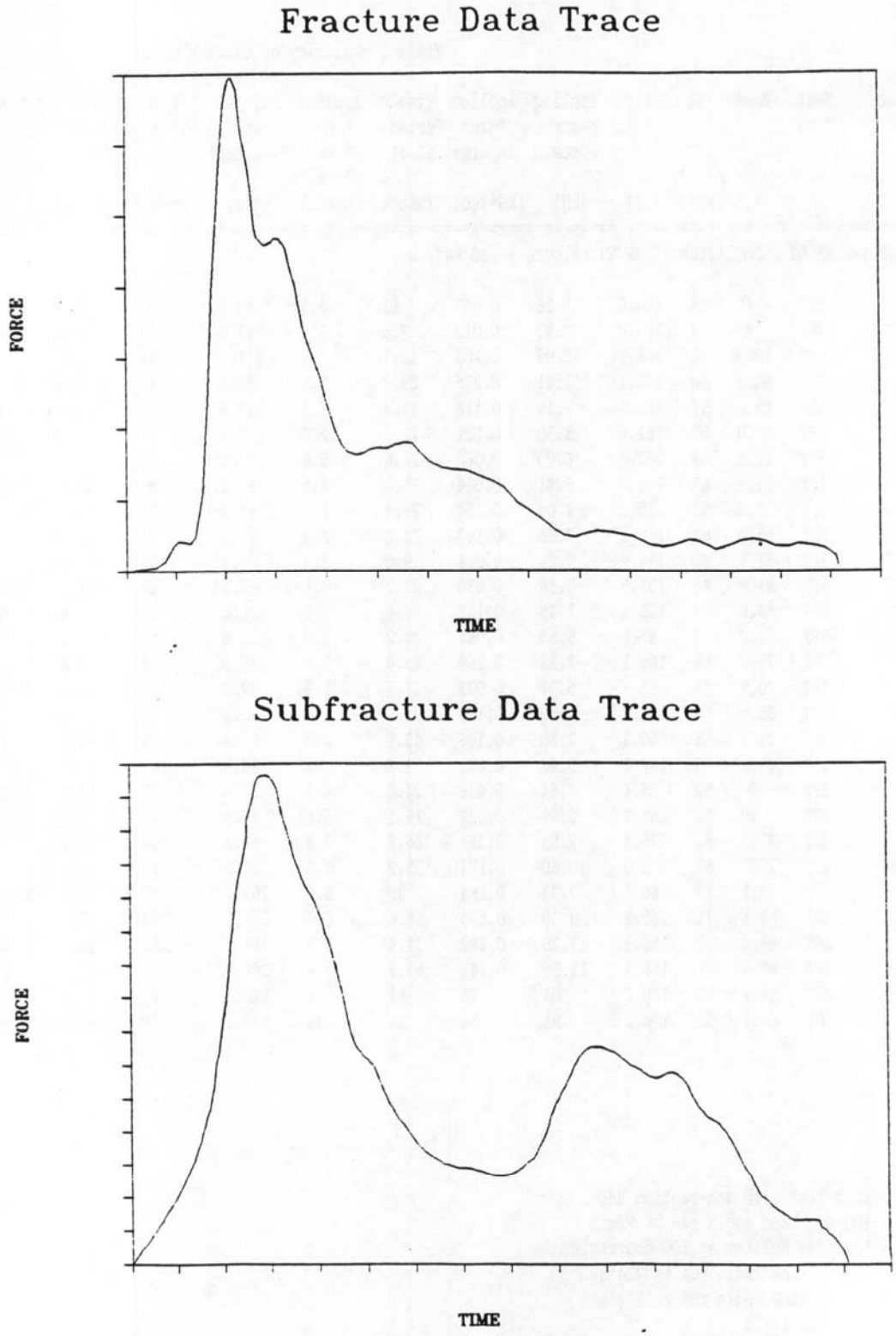

Figure 1. Comparison of fracture/subfracture data traces (Reference 5)

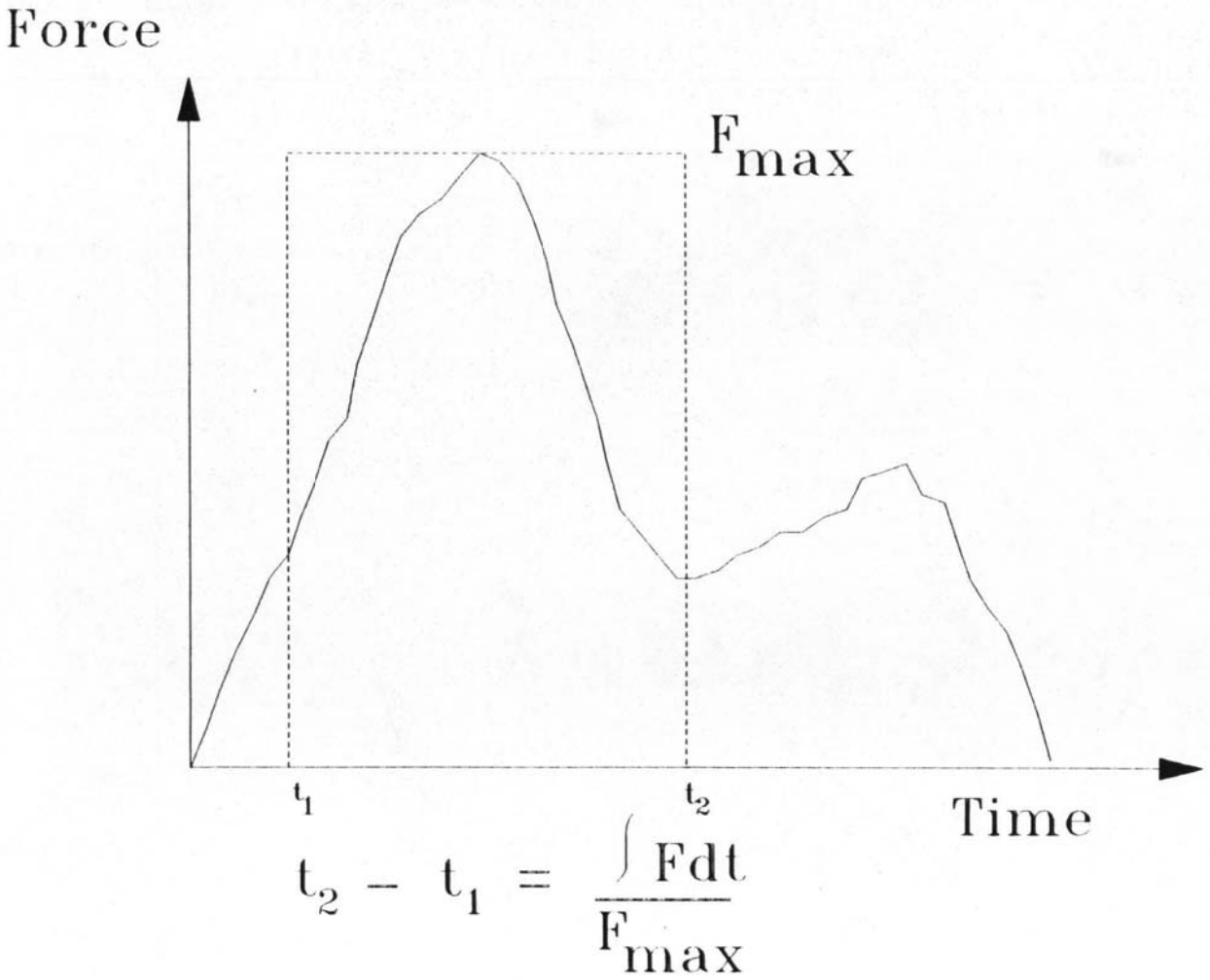

Figure 2. Definition of pulse duration using maximum femur force and integral of femur force

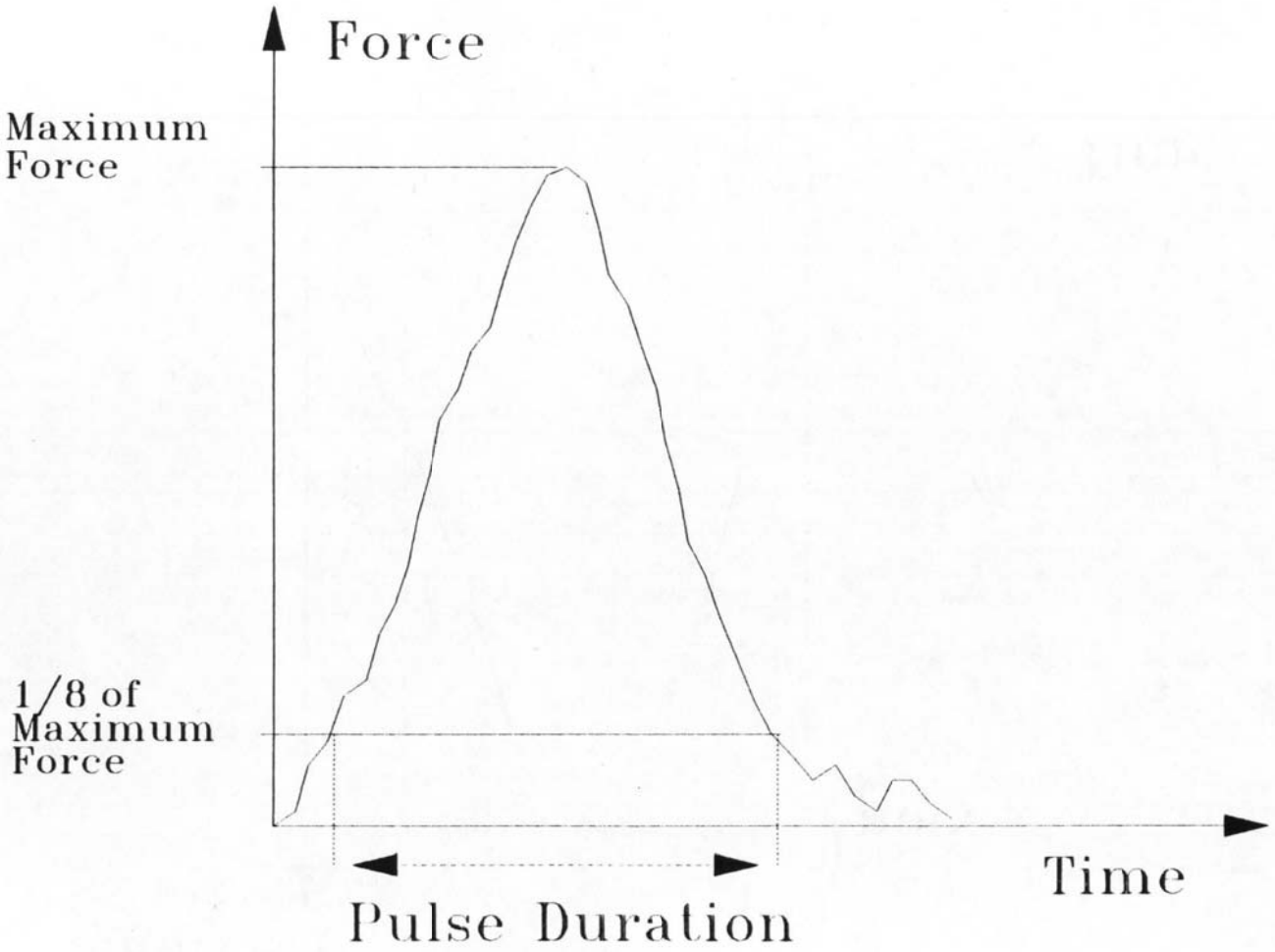

Figure 3. Definition of pulse duration using time at 1/8th of maximum applied femur force.

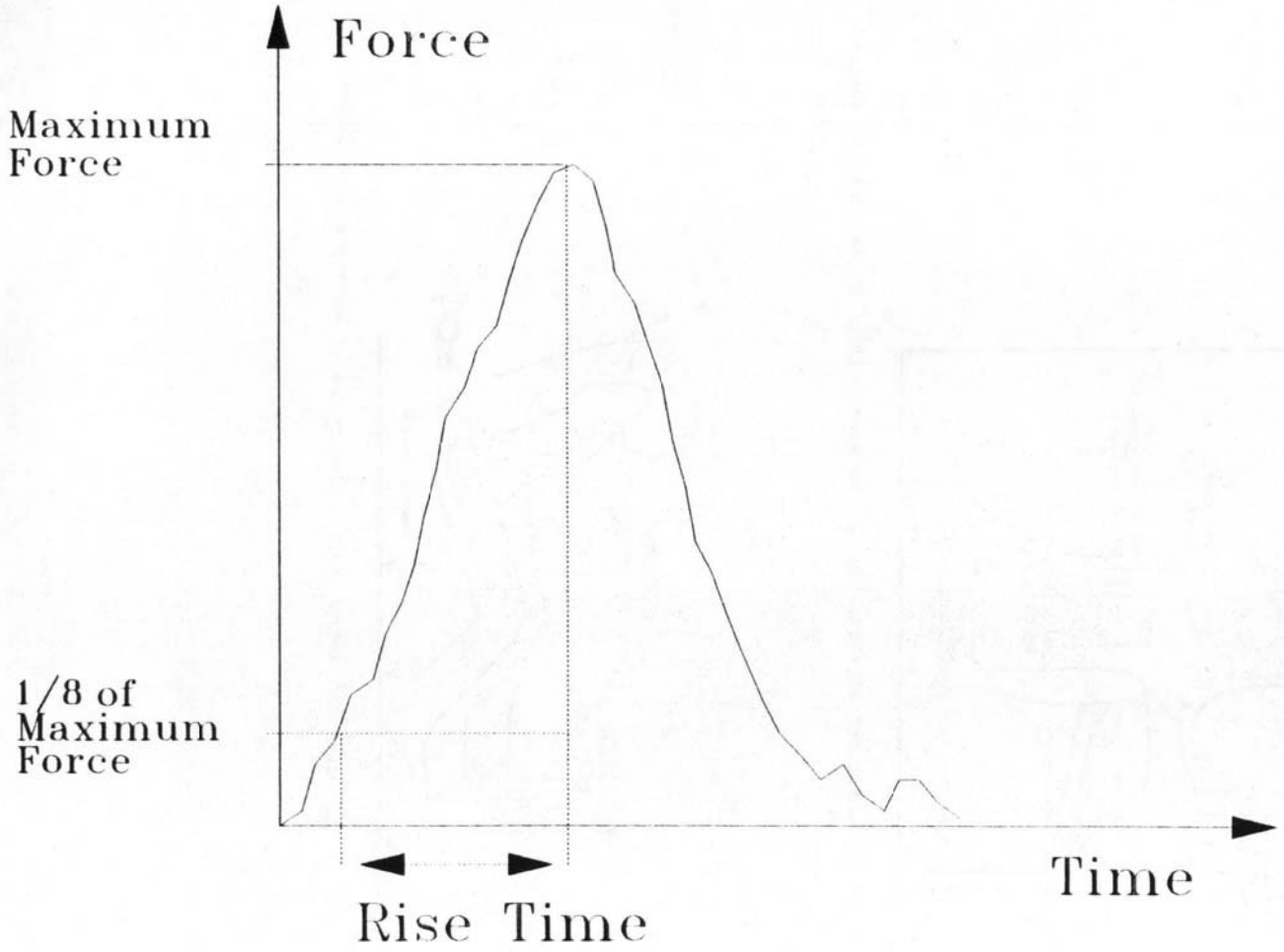

Figure 4. Definition of rise time using the difference between the time of maximum applied femur force and the time at 1/8th of the peak force

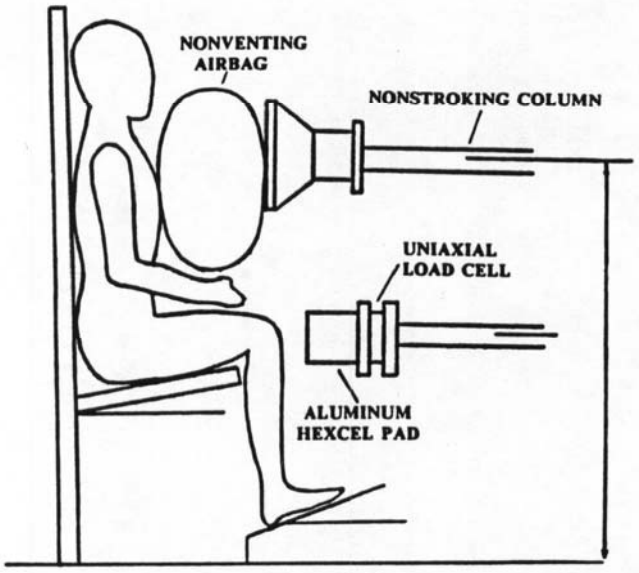

Figure 5. Experimental setup used in Reference 10 at Wayne State University

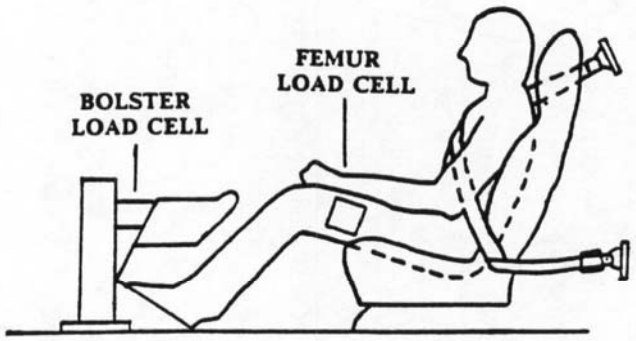

Figure 6. Experimental setup used in Reference 11 at Wayne State University

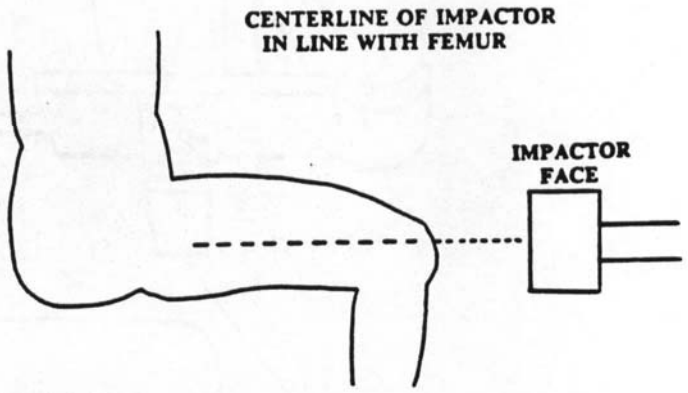

Figure 7. Experimental setup used in Reference 12 at Calspan Corporation

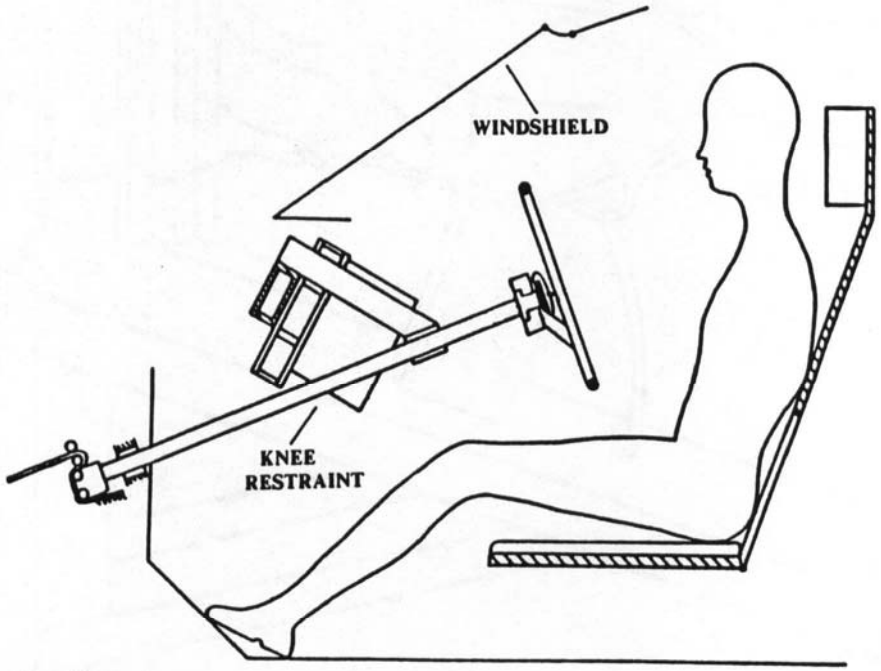

Figure 8. Experimental setup used in Reference 14 at the University of California at San Diego

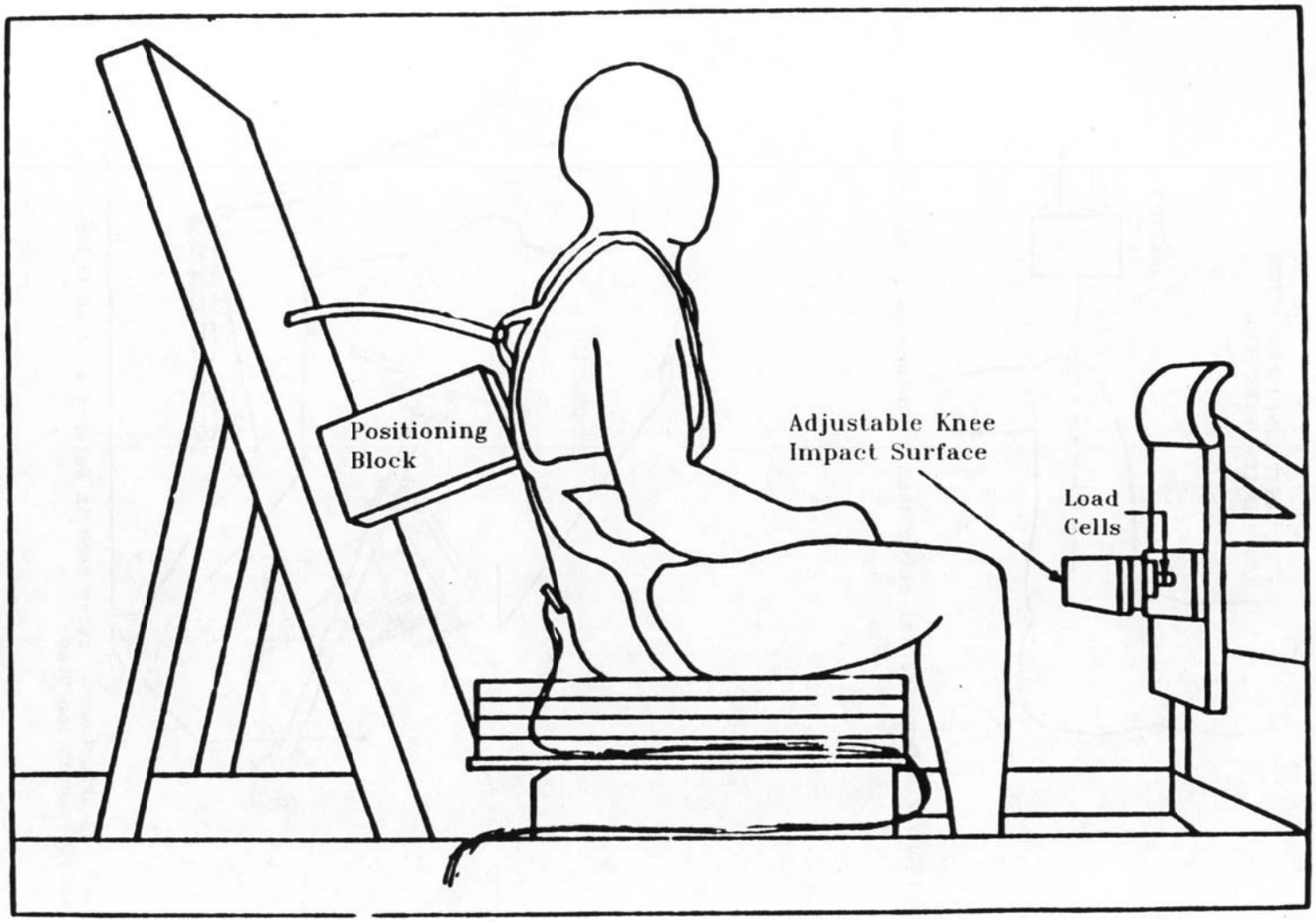

Figure 9. Experimental setup used in Reference 15 at the University of Michigan

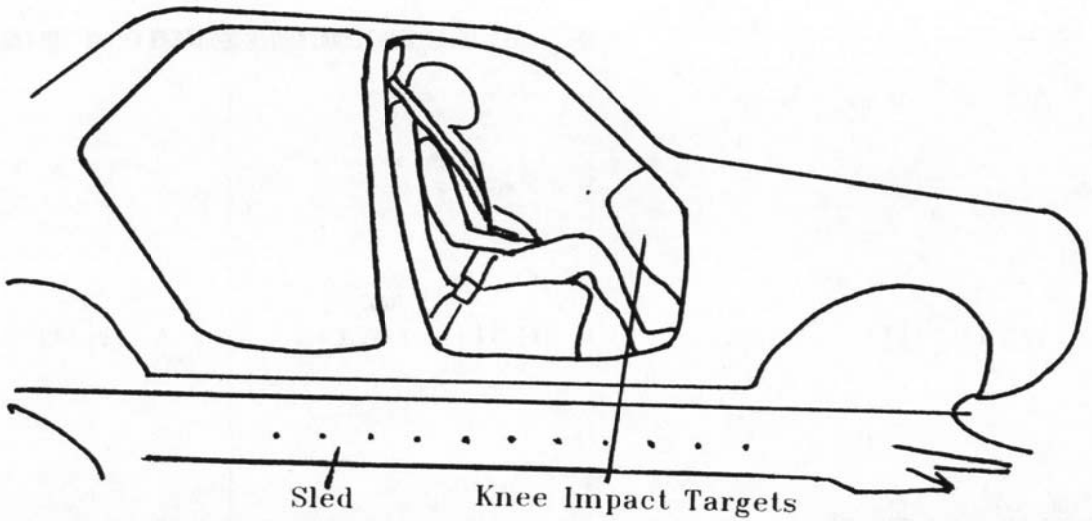

Figure 10. Experimental setup used in Reference 8 at the Peugeot-Renault Association

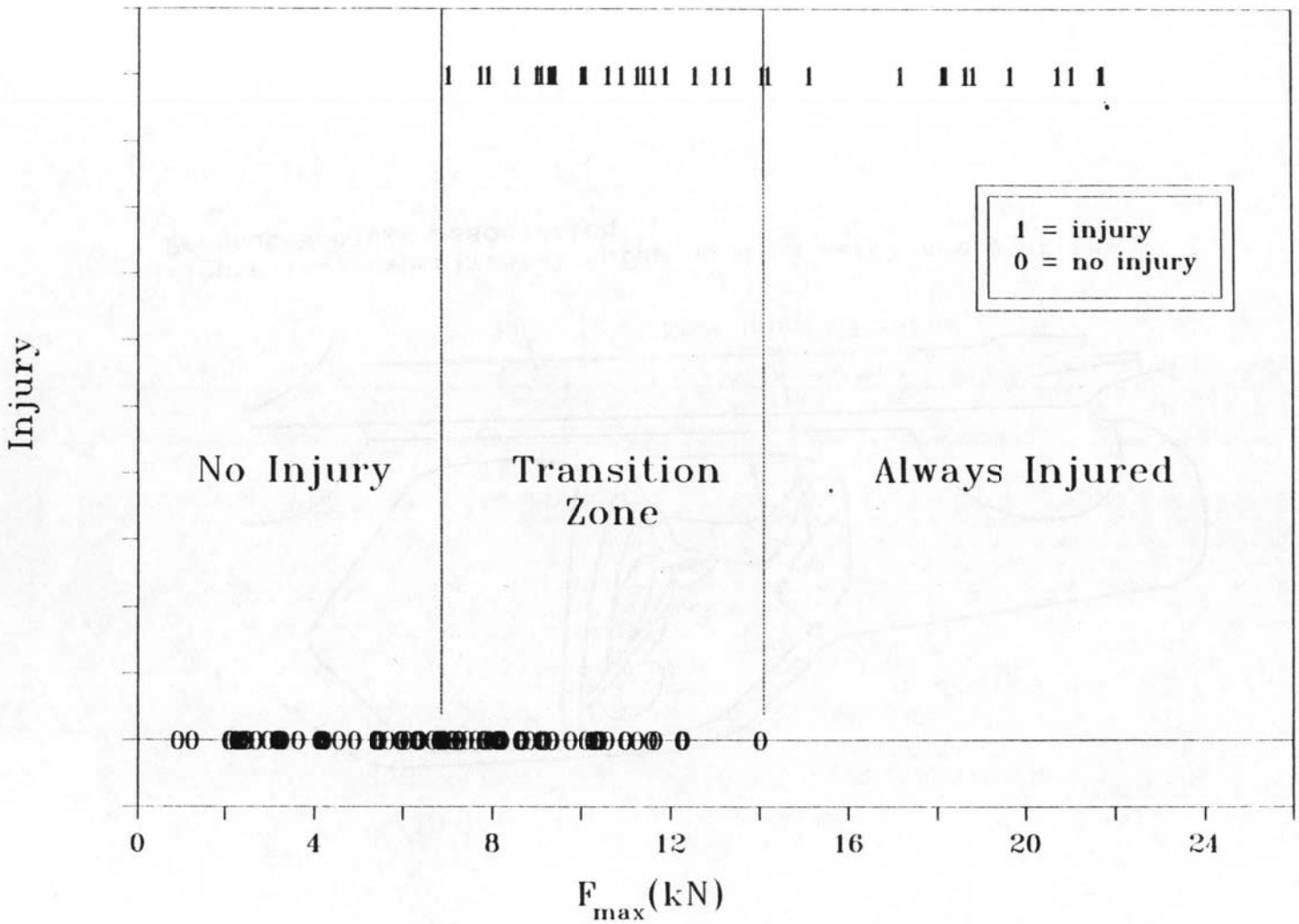

Figure 11. Injury/Non-Injury versus Maximum Applied Femur Force

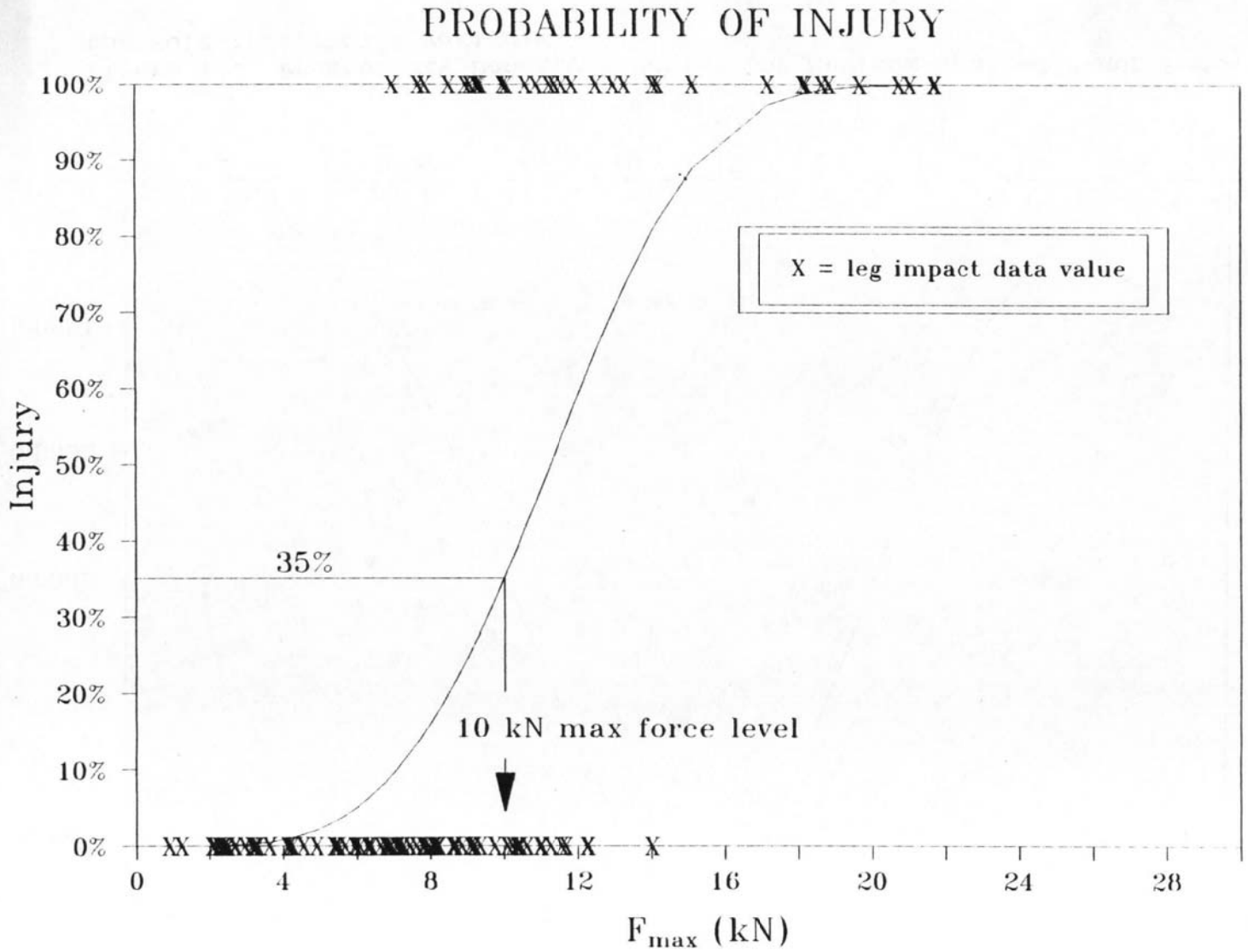

Figure 12. Probability of Injury as Function of Maximum Applied Femur Force

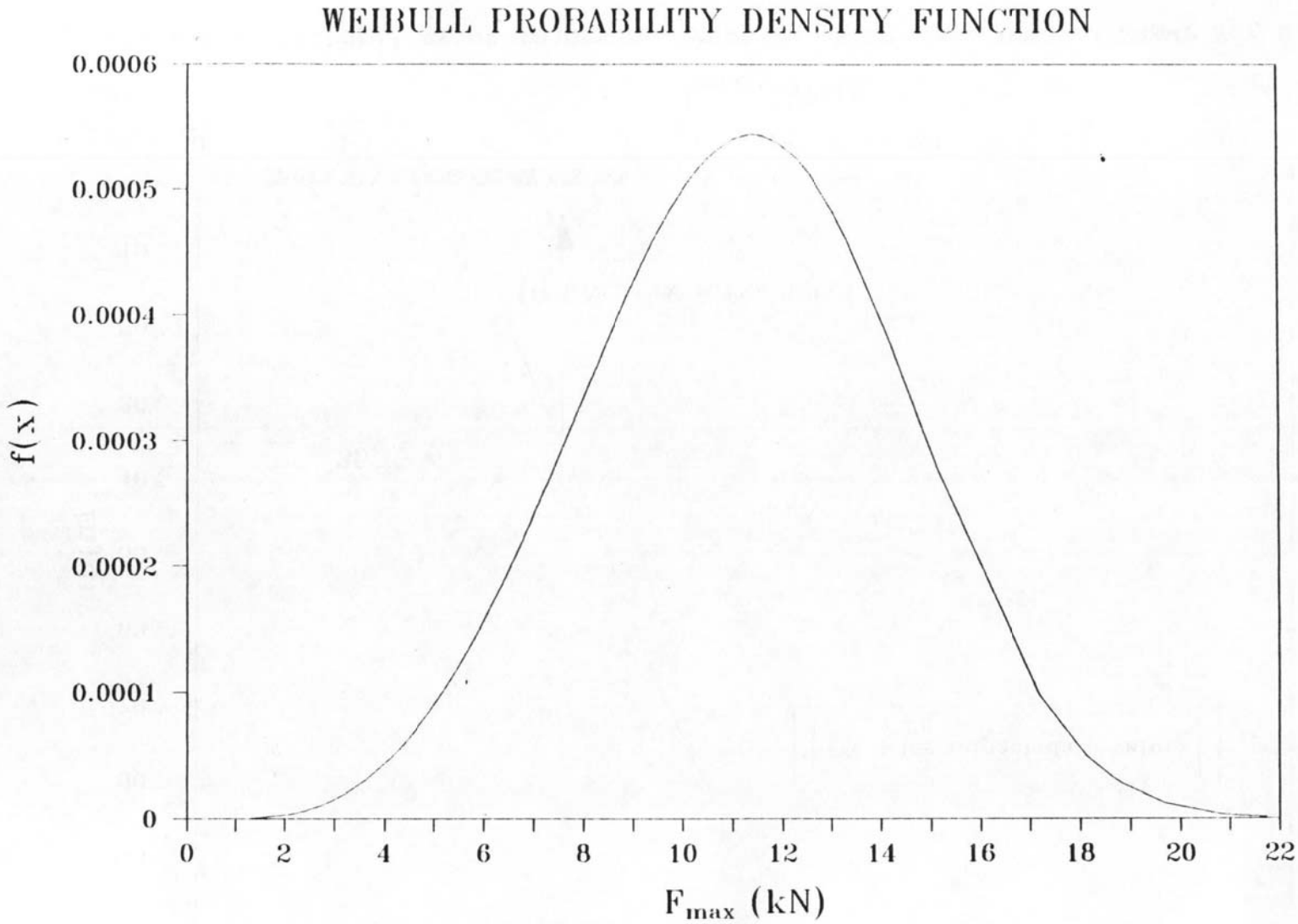

Figure 13. Probability Density Function for Maximum Applied Femur Force as the sole independent variable

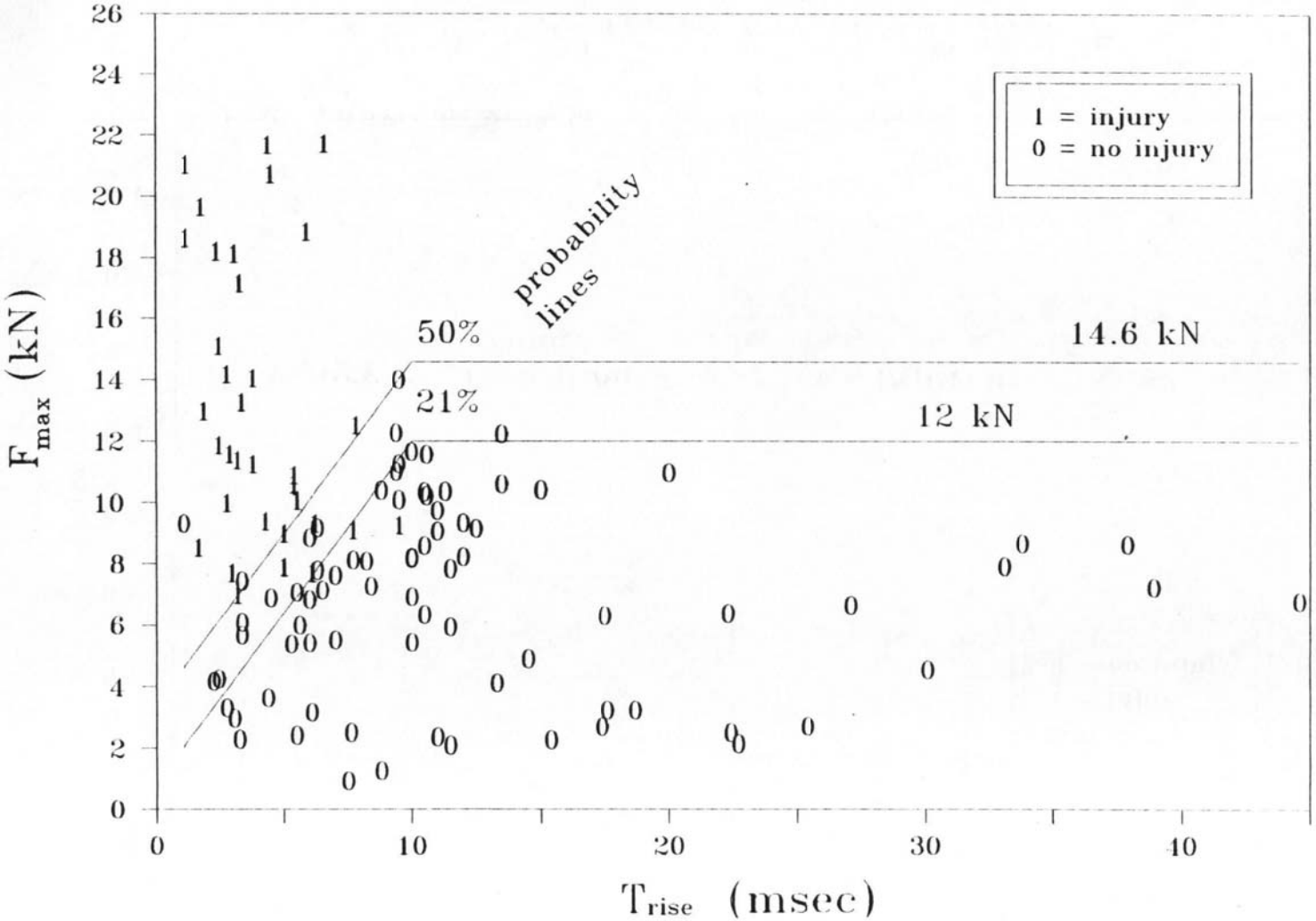

Figure 14. Injury/Non-Injury overlay on Maximum Applied Femur Force versus Femur Force Rise Time

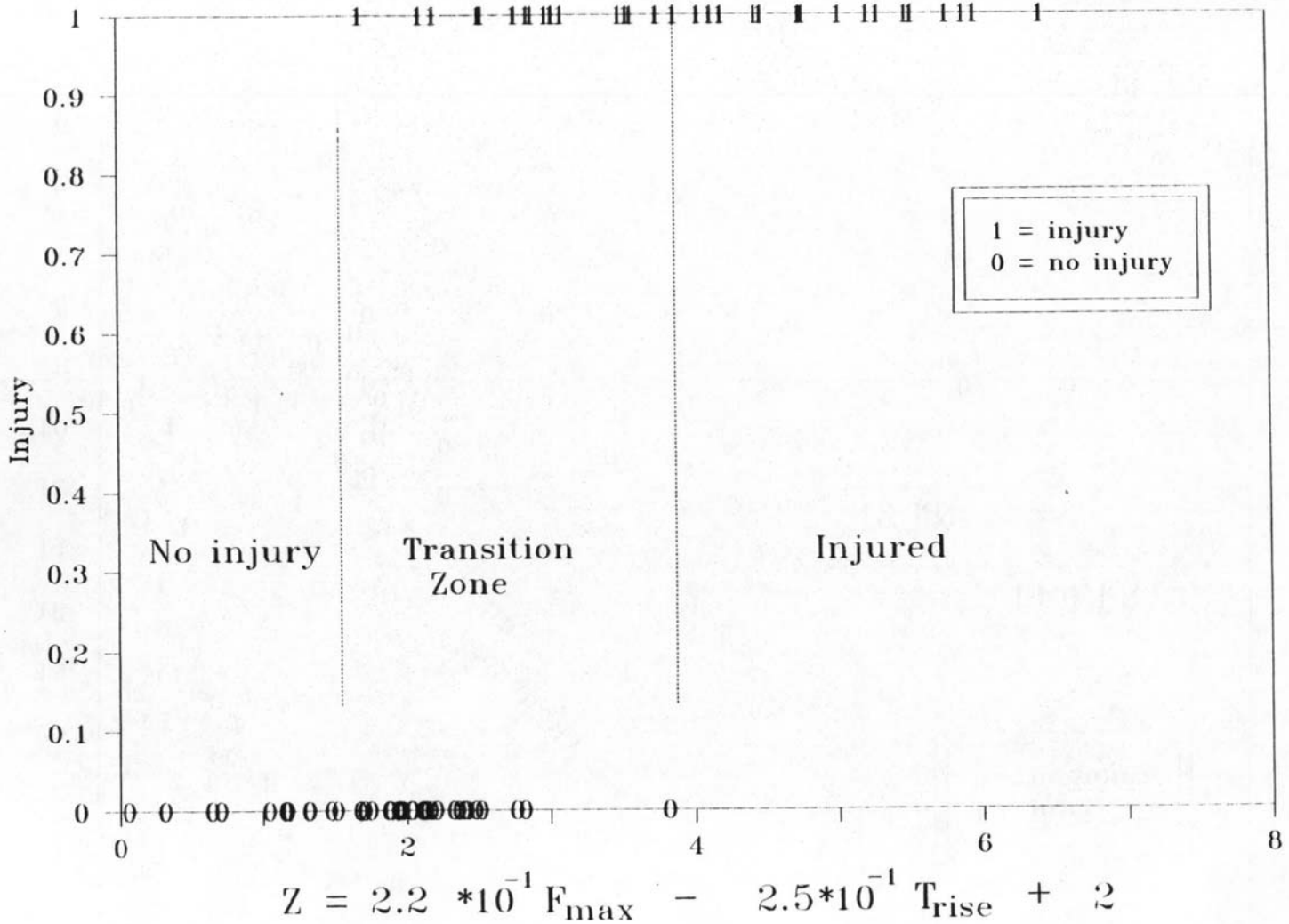

Figure 15. Injury/Non-Injury versus best linear combination of Maximum Applied Femur Force and Femur Rise Time (Rise Time <= 10 msec)

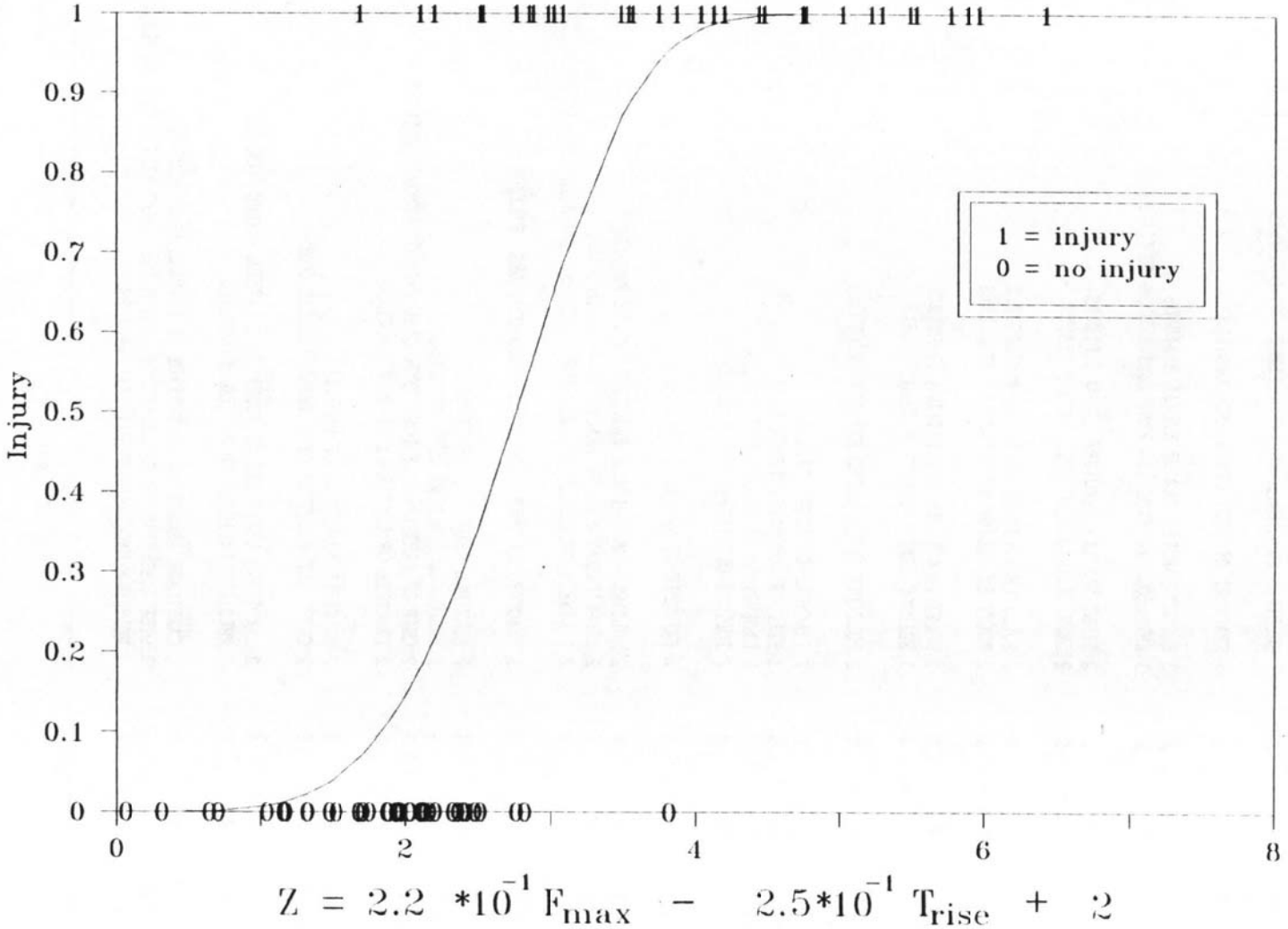

Figure 16. Probability of Injury as function of Maximum Applied Femur Force and Femur Rise Time (Rise Time <= 10 msec)

APPENDIX A

tstno	bodyrg	lesion	sysorg	ais	injtxt
W84024	K	F	S	2	RT KNEE FRACTURE OF PATELLA
W84024	T	F	S	3	MULTIPLE FRACTURES OF RIGHT FEMUR AND CONDYLES
W84124	T	F	S	3	FRACTURE OF LEFT FEMUR AND CONDYLES
C84129	K	G	M	2	BUCKET HANDLE TEAR OF MEDIAL MENISCUS
C84129	K	R	M	3	ANTERIOR CRUCIATE LIGAMENT RUPTURED ON MEDIAL SIDE
C84030	K	F	S	2	RIGHT PATELLA FRACTURED INTO 6 PIECES
C84130	K	F	S	2	LEFT PATELLA FRACTURED INTO 5 PIECES
C84031	K	F	S	2	MULTIPLE UNDISPLACED PATELLA FRACTURES
C84131	K	F	S	2	MULTIPLE UNDISPLACED PATELLA FRACTURES
C84032	K	F	S	2	MULTIPLE UNDISPLACED PATELLA FRACTURES
C84032	T	F	S	3	HEAD OF FEMUR FRACTURED TRANSVERSELY
C84132	K	F	S	2	MULTIPLE UNDISPLACED PATELLA FRACTURES
C84033	K	F	S	2	FRACTURE OF RIGHT PATELLA
C84033	T	F	S	3	FRACTURE OF RIGHT FEMUR HEAD
C84033	T	L	M	2	LACERATION OF TENSOR FACIA LATA
C84033	T	R	M	2	RUPTURE OF ILIOFEMORAL LIGAMENT
C84133	K	F	S	2	FRACTURE OF THE LEFT PATELLA
C84034	K	F	S	2	MULTIPLE UNDISPLACED FRACTURE OF THE PATELLA
C84034	P	F	S	2	DISPLACED CARTILAGE FRACTURES OF ACETABULUM
C84034	T	F	S	2 3	LINEAR UNDISPLACED CARTILAGE FRACTURES ABOVE INTERCONDYLAR FOSSA
C84134	T	F	S	3	FRACTURE OF BOTH EPICONDYLES AND CONDYLES OF FEMUR
C84035	K	F	S	2	MULTIPLE FRACTURES OF PATELLA
C84035	L	F	S	3	DISPLACED FRACTURE OF RIGHT TIBIA
C84035	K	G	S	2	CHIP OF CARTILAGE ON POST EROMEDIAL PART OF FEMORAL CONDYLE
C84035	P	F	S	2	FRACTURE OF CARTILAGE IN RIGHT ACETABULUM
C84135	K	F	S	2	MULTIPLE FRACTURES OF PATELLA
C84135	K	F	S	2	CARTILAGE FRACTURE OF LATERAL FEMORAL CONDYLE
C84036	K	A	S	2	CARTILAGE ABRASIONS ON SURFACE OF LATERAL FEMUR CONDYLE
C84036	K	F	S	2	MULTIPLE UNDISPLACED PATELLA FRACTURES
C84136	K	A	S	2	CARTILAGE ABRASIONS ON SURFACE OF LATERAL FEMUR CONDYLE
C84136	K	F	S	2	DISPLACED CHIP OF CARTILAGE ON POST-MEDIAL PART MEDIAL TIBIAL PLATEAU
C84136	K	F	S	2	MULTIPLE UNDISPLACED PATELLA FRACTURES

(Continued)

C85037 K	A	S	2 ABRASION OF POSTERIOR SURFACE OF PATELLA
C85037 L	F	S	2 SUBCAPITOL FRACTURE OF FIBULA
C85137 K	F	S	2 UNDISPLACED FRACTURE OF PATELLA
C85137 T	F	S	3 SUBCAPITOL FRACTURE OF FEMUR
C85038 T	F	S	3 DISPLACED FRACTURE AT BASE OF RIGHT FEMORAL NECK
C85138 P	F	S	2 UNDISPLACED FRACTURE ON THE ANTERIOR SUPERIOR PART OF ACETABULUM
C85040 K	F	S	2 STELLATE FRACTURE OF PATELLA
C85040 L	F	S	2 UNDISPLACED FRACTURE POSTERIOR PART OF HEAD OF FIBULA
C85040 T	F	S	3 DISPLACED INTERCONDYLAR Y FRACTURE SEPARATING MEDIAL & LATERAL CONDYLE
C85140 K	F	S	2 UNDISPLACED STELLATE FRACTURE OF PATELLA
C85140 L	F	S	2 COMPLETE SUPRACONDYLAR FRACTURE BELOW NECK OF FIBULA
C85140 T	F	S	3 DISPLACED INTERCONDYLAR Y FRACTURE SEPARATING MEDIAL & LATERAL CONDYLE
C85041 K	F	S	2 UNDISPLACED FRACTURE OF POSTEROMEDIAL PART OF PATELLA
C85041 T	F	S	3 INTERCONDYLAR FRACTURE DISPLACING MEDIAL AND LATERAL CONDYLES
C85041 T	F	S	3 FEMUR FRACTURE DISTAL TO LOAD CELL DISPLACING MULTIPLE FRAGMENTS FROM SHAFT
C85141 K	F	S	2 STELLATE UNDISPLACED FRACTURE OF PATELLA
C85141 L	F	S	2 UNDISPLACED FRACTURE OF TIBIA
C85141 T	F	S	3 SPIRAL FRACTURE IN DISTAL FEMUR
C85141 T	F	S	3 SUBCAPITAL FRACTURE. MULTIPLE FRACTURES ON FEMORAL NECK
C85141 T	F	S	3 UNDISPLACED INTERCONDYLAR FRACTURE
C85042 K	F	S	2 COMPLETE UNDISPLACED VERTICAL FRACTURE OF PATELLA
C85042 L	L	I	1 HORIZONAL LACERATION OF SKIN BELOW TIBIAL TUBEROSITY
C85042 T	F	S	3 COMPLETE FRACTURE OF DISTAL FEMUR
C85042 T	F	S	3 COMPLETE VERTICLE FRACTURE OF LATERAL CONDYLE
C85042 T	L	M	2 SLIGHT LACERATION OF BICEPS FEMORIS MUSCLE
C85042 T	L	M	2 SLIGHT LACERATION OF SEMIMEMBRANOSUS MUSCLE
C85142 K	F	S	2 STELLATE FRACTURE OF PATELLA
C85142 L	F	S	2 FRACTURE OF LATERAL PORTION OF TIBIAHEAD
C85142 L	F	S	2 MULTIPLE FRACTURES OF LATERAL SURFACE OF TIBIAL PLATEAU
C85142 L	L	I	1 HORIZONAL LACERATION OF SKIN BELOW TIBIAL TUBEROSITY
C85142 T	F	S	3 COMPLETE FRACTURE OF DISTAL FEMUR
C85142 T	F	S	3 COMPLETE INTERCONDYLER FRACTURE
C85142 T	L	M	2 LACERATION OF BICEPS FEMORIS MUSCLE
C85142 T	L	M	2 LACERATION OF SEMIMEMBRANOSUS MUSCLE
S86103 K	L	I	2 DEEP LACERATION OF MEDIAL LEFT KNEE TO COLLATERAL LIGAMENT
M80018 T	F	S	3 FRACTURE OF THE NECK OF THE FEMUR
M80018 T	F	S	3 FRACTURES OF THE CONDYLES OF THE FEMUR

(Continued)

M80118	T	F	S	3 FRACTURE OF THE NECK OF THE FEMUR
M80118	T	F	S	3 FRACTURE OF THE SHAFT OF THE FEMUR
M80118	T	F	S	3 CRACKING OF THE CONDYLES
M80118	K	F	S	2 FRACTURE OF THE PATELLA
M80020	T	F	S	3 FRACTURE OF THE NECK OF THE FEMUR
M80020	T	F	S	3 FRACTURE OF THE SHAFT OF THE FEMUR
M80020	T	F	S	3 FRACTURE OF THE MEDIAL CONDYLE OF THE FEMUR
M80120	T	F	S	3 FRACTURE OF THE NECK OF THE FEMUR
M80120	T	F	S	3 FRACTURE OF THE SHAFT OF THE FEMUR
M80120	T	F	S	3 FRACTURE OF THE MEDIAL CONDYLE OF THE FEMUR
M80021	T	F	S	3 FRACTURE OF THE MEDIAL CONDYLE OF THE FEMUR
M80021	T	F	S	3 FRACTURE OF THE SHAFT OF THE FEMUR
M80021	K	F	S	2 FRACTURE OF THE PATELLA
M80121	T	F	S	3 FRACTURE OF THE FEMORAL CONDYLES
M80121	K	F	S	2 FRACTURE OF THE PATELLA
M80121	P	F	S	2 FRACTURE OF THE ACETABULUM
F0280	T	F	S	3 FRACTURE OF THE RIGHT CONDYLE
F0280	K	F	S	2 FRACTURE OF THE RIGHT PATELLA
F1280	K	F	S	2 FRACTURE OF THE LEFT PATELLA
F0281	T	F	S	3 FRACTURE OF THE NECK OF THE RIGHT FEMUR
F0281	K	F	S	2 FRACTURE OF THE RIGHT PATELLA
F1281	K	F	S	2 FRACTURE OF THE LEFT PATELLA
F0294	T	F	S	3 FRACTURE OF THE DISTAL PART OF THE RIGHT FEMUR
F1296	T	F	S	3 FRACTURE OF THE RIGHT PART OF THE LEFT FEMUR
F1296	T	F	S	3 FRACTURE OF THE SUB-CONDYLE OF THE LEFT FEMUR

tstno = Test Number

bodyrg = Body Region
- K = Knee
- T = Thigh
- L = Leg
- P = Pelvis/Hip

lesion = Type of Injury
- F = Fracture
- L = Laceration
- G = Detachment/Separation
- A = Abrasion
- R = Rupture

sysorg = Injured Organ
- S = Skeletal
- M = Muscle
- I = Integumentary

ais = Abbreviated Injury Scale (1980 Revision)

APPENDIX B

It is the objective of this appendix to show the data set of Table 1 does not support a bivariate injury model composed of maximum applied femur force and primary pulse duration. A plot of the maximum applied femur force as a function of the primary pulse duration of the applied femur force is exhibited in Figure B1 for this data set. The solid line is Viano's proposed Femur Injury Criteria. [7] There does not appear to be a good separation of injury for this data set. Is the current data set radically different from the data set used in Reference 7 ? Figure B2 is a graph of the unembalmed cadaver impact data from Reference 7. Again, there does not appear to be a good separation of injury/non-injury. The cadaver injury data of Reference 7 is next analyzed by multiple discriminant analysis.

The data input for the SAS Discriminant Analysis came from the cadaver
impact information in Reference 7 (the data exhibited in Figure B2). Figure B3 shows the results of this analysis. Basically, the best -- in the Discriminant Analysis sense -- linear combination of maximum applied femur force and primary pulse duration of the applied femur force does not do a good job of separating injury/non-injury for the Reference 7 data set.

There may be many reasons for the lack of separation of injury for the 112 experiments of Table 1 using the Viano criterion. For example, the pulse duration definition methodology, data processing procedures, and/or data quality may be disparate.

A logical next step would be to determine whether the model generated in this paper -- using the 112 experiments of Table 1 -- would do a robust job of separating injury from non-injury for the Reference 7 data. The data of Reference 7 are in summary form, i. e., Reference 7 does not have the individual force-time curves for the leg impact experiments. We did not use the Reference 7 data to test the model generated in this paper because we could not find values for rise time.

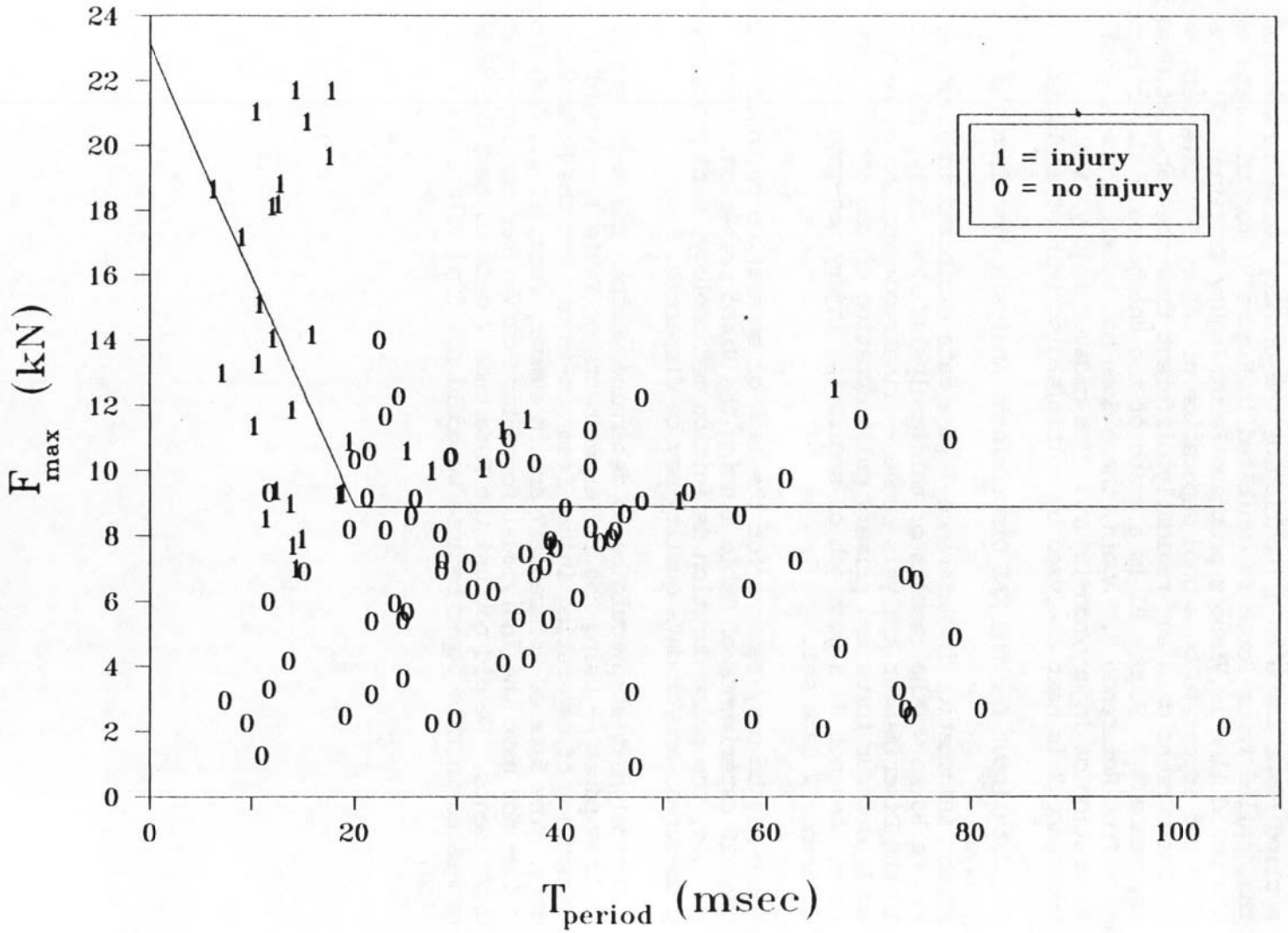

Figure B1. Injury/Non-Injury overlay on Applied Femur Force versus Primary Pulse Duration

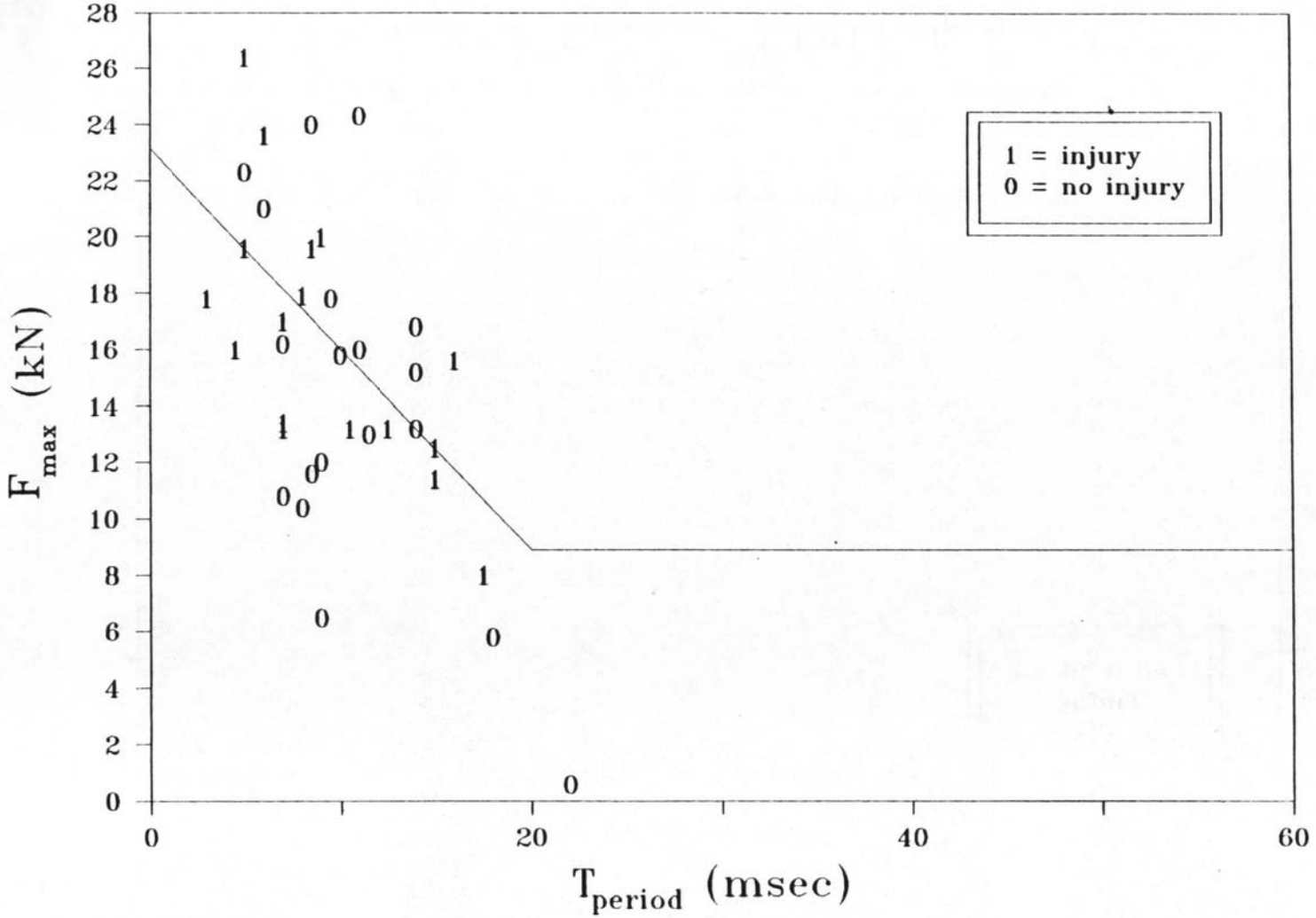

Figure B2. Overlay of Injury/Non-Injury from Reference 7 on Applied Femur Force versus Primary Pulse Duration

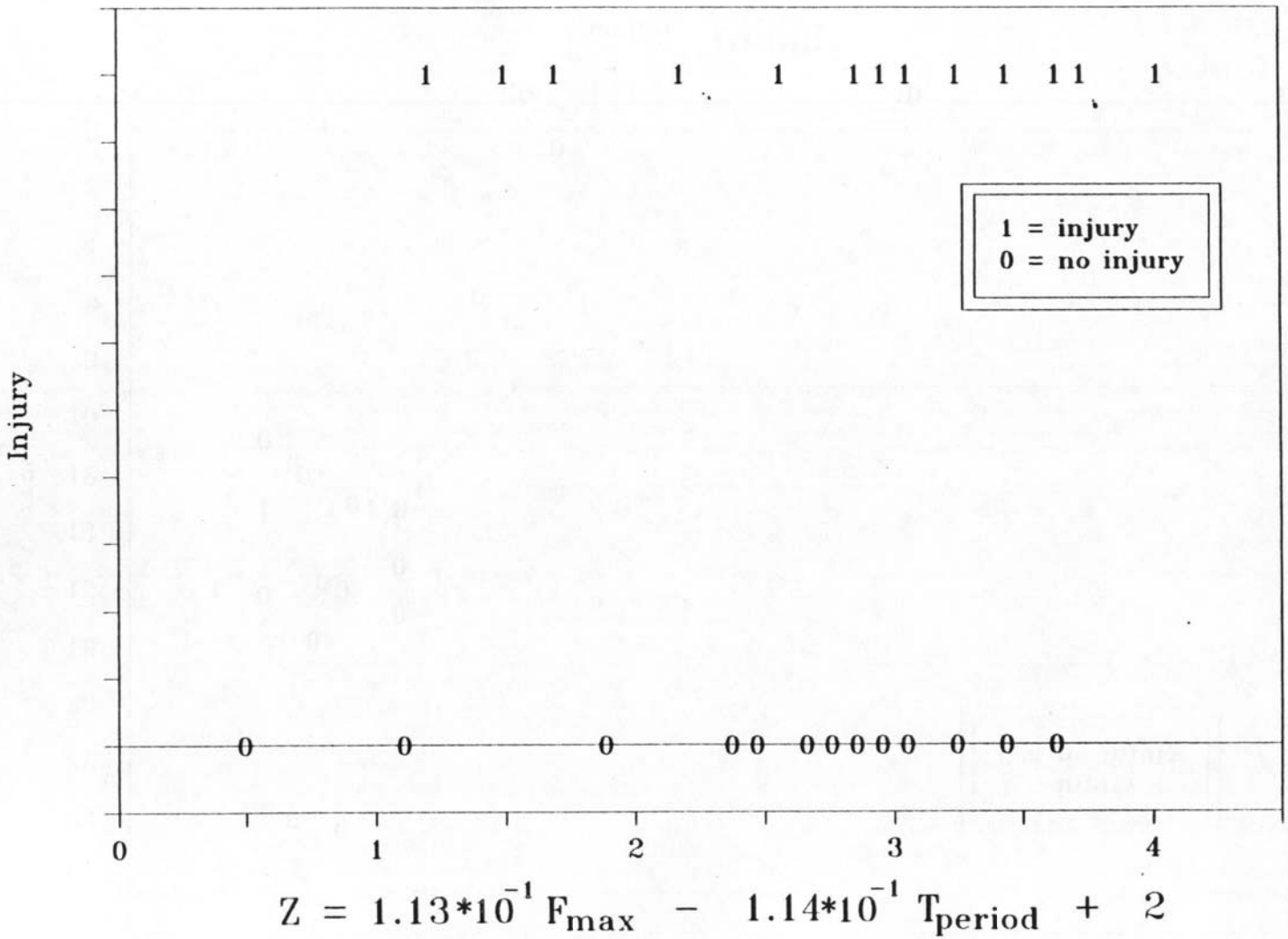

Figure B3. Injury/Non-Injury From Reference 7 versus best linear combination of Applied Femur Force and Primary Pulse Duration